R. & M. No. 2885
(15,096)
A.R.C. Technical Report

MINISTRY OF SUPPLY

AERONAUTICAL RESEARCH COUNCIL
REPORTS AND MEMORANDA

Multhopp's Subsonic Lifting-Surface Theory of Wings in Slow Pitching Oscillations

By

H. C. GARNER, B.A.,
of the Aerodynamics Division, N.P.L.

LONDON: HER MAJESTY'S STATIONERY OFFICE
1956
THIRTEEN SHILLINGS NET

Multhopp's Subsonic Lifting-Surface Theory of Wings in Slow Pitching Oscillations

By

H. C. Garner, B.A.,
of the Aerodynamics Division, N.P.L.

Reports and Memoranda No. 2885
July, 1952

Summary.—A draft of this theory was completed by H. Multhopp during 1950, before he left the Ministry of Supply. It has been edited by the writer, who is responsible for the calculated examples.

This report is an extension of Multhopp's subsonic lifting-surface theory (Ref. 1) from steady flow to harmonic pitching oscillations of low frequency. The method is applicable to wings of arbitrary plan-form.

The basis of the method is to calculate the local lift and pitching moment at a number of chordwise sections from a set of linear equations satisfying the downwash conditions at two points of each section. By neglecting terms of second order in frequency, the oscillatory problem is related to the corresponding steady one with changed boundary conditions. The evaluation of these conditions involves chordwise integrations, which require two new influence functions. Complete tables of these functions as well as the original functions i and j, occurring in steady motion (Ref. 1), are obtainable from the Aerodynamics Division, National Physical Laboratory (Ref. 11). With the aid of these tables the derivatives of lift and pitching moment become calculable by a straightforward routine. The limitations imposed by assuming only two terms in the chordwise loading cannot be evaluated at this stage. The theory is easily generalized to include any number of chordwise terms, but each additional term introduces two further influence functions.

The theory is outlined in sections 2 to 5. Section 6 describes calculations of pitching derivatives for circular, arrowhead and a family of delta wings; promising comparisons are obtained, when the number of spanwise terms is varied. In sections 7 and 8 these results are compared with other theories; a development of vortex-lattice theory (Ref. 5) is shown to give satisfactory agreement, and the deficiencies of a purely steady theory are evaluated. The available wind-tunnel data for oscillating wings of the selected plan-forms are discussed in section 9. The theory is remarkably consistent with the pitching derivatives measured at low speeds and predicts fairly well the effect of compressibility up to a Mach number of about 0·9. Appendix II gives instructions for the computer.

1. *Introduction.*—In Ref. 1 (1950) Multhopp has developed a method of calculating the local lift and pitching moment on wings of any plan-form in subsonic steady flow. The method is based on the acceleration potential and represents the lifting surface by a plane continuous sheet of doublets extending over the plan-form. It makes the usual assumptions that the wing is infinitely thin in inviscid potential flow, and neglects terms of the second order in incidence, camber and perturbations of velocity.

The method, as it stands, is capable of dealing with the oscillatory problems of rolling and plunging in the limiting case of small frequency. For there is no distinction between the steady stability derivatives and the limiting oscillatory ones, so long as the in-phase aerodynamic loading vanishes with frequency. However pitching motion is not of this type and calls for a special adaptation of method to deduce the first order effects of frequency.

The important derivative from pitching oscillations is the out-of-phase pitching moment, which constitutes the aerodynamic damping of the motion. Hence 'lifting-line' aerofoil theory does not give a very fruitful treatment of the problem. The first suggested routine for applying lifting-surface theory to oscillating wings came from W. P. Jones[2] (1946). His method is a development of the steady vortex-lattice theory[3] (Falkner, 1943) and may be applied to wings of any plan-form. The theory includes an arbitrary non-zero value of the frequency parameter, but it is unsuitable for oscillations of low frequency. Following Ref. 2, aerodynamic flutter derivatives for a delta wing have been calculated in Ref. 4 (Lehrian, 1951). Miss Lehrian[5] has also modified the theory of Ref. 2 to permit the calculation of stability derivatives of low frequency. Her results are compared with those of the present method.

The limitations of Multhopp's steady theory (Ref. 1) and other standard ones, including Falkner's vortex-lattice theory (Ref. 3), have been discussed by the writer in Ref. 6 (1951). Of these methods Ref. 1 is considered to be the most reliable, though the flexibility of the vortex lattice permits the treatment of a wider range of problems, including pitching and rolling oscillations of high frequency. The extension of Ref. 1 to pitching oscillations of low frequency should provide reliable routine estimations of theoretical stability derivatives at sub-critical Mach numbers. The method is particularly economical for swept wings of moderately small aspect ratios.

At present there is limited information on oscillatory pitching derivatives ; but it is known that the values in steady rotation are usually appreciably different. There exist independent solutions for an oscillating circular plate due to Schade and Krienes[7] and to Kochin[8]. The circular aerofoil has therefore been chosen as one of the present examples.

The other examples are derived from Ref. 6, Fig. 1, and are included in the programme of oscillatory tests at the N.P.L. These comprise the arrowhead Wing 9 ($A = 1\cdot 32$) and three delta wings in the family $(\delta, \lambda) = (0, 1/7)$, *i.e.*, Wings 0, 1, 2 with aspect ratios of $1\cdot 2$, 2, 3 respectively. Wings 0 and 9 have been tested at several frequencies at low speeds. A half-model of Wing 2 has been tested over a range of subsonic Mach number.

Mention should be made of other theories, which are not considered in relation to the present calculations. The most promising development of the 'lifting-line' aerofoil theory is perhaps that due to Reissner[9] (1947). There has appeared recently a new theory giving numerical solutions for oscillating rectangular and triangular wings of low aspect ratio[10] (Lawrence and Gerber, 1952). W. P. Jones[17] (1951) has considered the problem of oscillating wings in compressible flow, and has discussed the effects of frequency at a Mach number of $0\cdot 7$.

2. *General Theory*.—It is convenient to take rectangular co-ordinate axes referred to the leading edge of the central section of the wing. Let the x-axis coincide with the horizontal direction of undisturbed flow relative to the wing, the y-axis point to starboard and the z-axis upwards. The wing is assumed to have zero thickness and the local velocity to have components $(U + u, v, w)$, where U is the undisturbed speed and the ratios $(u/U)^2$, $(v/U)^2$, $(w/U)^2$ are negligible compared with u/U, v/U, w/U. This implies that the wing has small camber and twist and oscillates with small amplitude.

Then, in the absence of viscous forces and heat transfer, Euler's equations of motion may be expressed in their linearized form

$$\left.\begin{aligned} \frac{\partial u}{\partial t} + U\frac{\partial u}{\partial x} + \frac{1}{\rho}\frac{\partial p}{\partial x} &= 0 \\ \frac{\partial v}{\partial t} + U\frac{\partial v}{\partial x} + \frac{1}{\rho}\frac{\partial p}{\partial y} &= 0 \\ \frac{\partial w}{\partial t} + U\frac{\partial w}{\partial x} + \frac{1}{\rho}\frac{\partial p}{\partial z} &= 0 \end{aligned}\right\} \qquad \ldots \qquad (1)$$

and the equation of continuity becomes

$$\frac{\partial \rho}{\partial t} + U\frac{\partial \rho}{\partial x} + \rho\left(\frac{\partial u}{\partial x} + \frac{\partial v}{\partial y} + \frac{\partial w}{\partial z}\right) = 0\,. \qquad (2)$$

In the absence of shock-waves, the isentropic relation between the pressure p and the density ρ

$$\frac{p}{\rho^{\gamma}} = \text{constant}$$

is assumed, and the speed of sound, a, is given by

$$a^2 = \frac{dp}{d\rho} = \frac{\gamma p}{\rho}\,. \qquad (3)$$

It may be shown that the variation in a^2 is of order, Uu and is negligible in combination with terms of order u/U in the linearized equations. Similarly ρ may be regarded as constant. On writing the differential dp/ρ of Euler's equations as the differential of the enthalpy I,

$$I - I_{\infty} = \frac{p - p_{\infty}}{\rho}\,, \qquad (4)$$

where the subscript ∞ represents the undisturbed flow.

Thus the equations of motion are transformed into

$$\left.\begin{aligned} \left(\frac{\partial}{\partial t} + U\frac{\partial}{\partial x}\right)u + \frac{\partial I}{\partial x} &= 0 \\ \left(\frac{\partial}{\partial t} + U\frac{\partial}{\partial x}\right)v + \frac{\partial I}{\partial y} &= 0 \\ \left(\frac{\partial}{\partial t} + U\frac{\partial}{\partial x}\right)w + \frac{\partial I}{\partial z} &= 0 \end{aligned}\right\} \qquad (5)$$

and the equation of continuity into

$$\frac{1}{a_{\infty}^2}\left(\frac{\partial}{\partial t} + U\frac{\partial}{\partial x}\right)I + \frac{\partial u}{\partial x} + \frac{\partial v}{\partial y} + \frac{\partial w}{\partial z} = 0\,, \qquad (6)$$

where a_{∞}^2 is a constant, and the operator $(\partial/\partial t + U\,\partial/\partial x)$ is identified with differentiation along a streamline. By applying this operator to equation (6) and taking the derivatives of u, v, w from equation (5), it follows that

$$\frac{1}{a_{\infty}^2}\left(\frac{\partial}{\partial t} + U\frac{\partial}{\partial x}\right)^2 I - \frac{\partial^2 I}{\partial x^2} - \frac{\partial^2 I}{\partial y^2} - \frac{\partial^2 I}{\partial z^2} = 0\,,$$

i.e.,

$$\frac{\partial^2 I}{\partial x^2} + \frac{\partial^2 I}{\partial y^2} + \frac{\partial^2 I}{\partial z^2} = \left(\frac{1}{a_{\infty}}\frac{\partial}{\partial t} + M\frac{\partial}{\partial x}\right)^2 I\,, \qquad (7)$$

where the Mach number $M = U/a_{\infty}$.

If I is periodic of frequency ω, (7) becomes the real part of a complex equation, which may be divided throughout by a factor $e^{i\omega t}$ to give a differential equation for the complex amplitude of I. To avoid complex terms in this equation, let

$$I(x, y, z, t) = \mathscr{R}\left[\bar{I}(x, y, z)\exp\{i\omega(t + \lambda x)\}\right], \qquad (8)$$

where λ remains to be chosen. Then

$$\left(\frac{1}{a_\infty}\frac{\partial}{\partial t} + M\frac{\partial}{\partial x}\right)^2 I = \mathscr{R}\left\{\left[M^2\frac{\partial^2 \bar{I}}{\partial x^2} + 2i\omega M\frac{\partial \bar{I}}{\partial x}\left(\frac{1}{a_\infty} + M\lambda\right)\right.\right.$$

$$\left.\left. - \omega^2 \bar{I}\left(\frac{1}{a_\infty} + M\lambda\right)^2\right]\exp\{i\omega(t + \lambda x)\}\right\}$$

$$\frac{\partial^2 I}{\partial x^2} = \mathscr{R}\left\{\left(\frac{\partial^2 \bar{I}}{\partial x^2} + 2i\omega\lambda\frac{\partial \bar{I}}{\partial x} - \omega^2\lambda^2\bar{I}\right)\exp\{i\omega(t + \lambda x)\}\right\}$$

$$\frac{\partial^2 I}{\partial y^2} = \mathscr{R}\left\{\frac{\partial^2 \bar{I}}{\partial y^2}\exp\{i\omega(t + \lambda x)\}\right\}$$

$$\frac{\partial^2 I}{\partial z^2} = \mathscr{R}\left\{\frac{\partial^2 \bar{I}}{\partial z^2}\exp\{i\omega(t + \lambda x)\}\right\}.$$

On putting these expressions into equation (7),

$$(1 - M^2)\frac{\partial^2 \bar{I}}{\partial x^2} + \frac{\partial^2 \bar{I}}{\partial y^2} + \frac{\partial^2 \bar{I}}{\partial z^2} = 2i\omega\frac{\partial \bar{I}}{\partial x}\left[M\left(\frac{1}{a_\infty} + M\lambda\right) - \lambda\right] - \omega^2\bar{I}\left[\left(\frac{1}{a_\infty} + M\lambda\right)^2 - \lambda^2\right].$$

By choosing

$$\lambda = \frac{M}{a_\infty(1 - M^2)} = \frac{1}{U}\frac{M^2}{1 - M^2}, \qquad (9)$$

the complex amplitude $\bar{I}$ is given by the real differential equation

$$(1 - M^2)\frac{\partial^2 \bar{I}}{\partial x^2} + \frac{\partial^2 \bar{I}}{\partial y^2} + \frac{\partial^2 \bar{I}}{\partial z^2} + \frac{\omega^2 M^2}{U^2(1 - M^2)}\bar{I} = 0. \qquad (10)$$

If the oscillation is slow enough and the Mach number not too near unity, *i.e.*, if the non-dimensional parameter

$$\frac{\omega\bar{c}M}{U(1 - M^2)} << 1,$$

the last term in equation (10) may be ignored and $\bar{I}$ satisfies

$$(1 - M^2)\frac{\partial^2 \bar{I}}{\partial x^2} + \frac{\partial^2 \bar{I}}{\partial y^2} + \frac{\partial^2 \bar{I}}{\partial z^2} = 0, \qquad (11)$$

which may be simplified to Laplace's equation by the Prandtl-Glauert transformation to new co-ordinates

$$[x, y\sqrt{(1 - M^2)}, z\sqrt{(1 - M^2)}].$$

From equation (4), the load per unit area is

$$(\Delta p) = \rho(\Delta I) = \tfrac{1}{2}\rho U^2 l, \qquad (12)$$

where Δ denotes the difference between the upper and lower surfaces of the wing, which may be assumed to lie in the plane $z = 0$. Let $\bar{l}$ be the complex amplitude of the non-dimensional oscillating load, l; and define $\bar{I}$ such that

$$\left.\begin{aligned} &\text{on the upper surface } \bar{I}(x', y', +0) = -\tfrac{1}{4}U^2\bar{l}(x', y') \\ &\text{on the lower surface } \bar{I}(x', y', -0) = +\tfrac{1}{4}U^2\bar{l}(x', y') \end{aligned}\right\} \quad \ldots \quad (13)$$

Thus the field of $\bar{I}$ is equivalent to the field of doublets of strength $(\Delta\bar{I})$ and axis in the positive z-direction distributed over the plan-form S. The standard solution of the generalized Laplace's equation (11) is

$$\bar{I}(x, y, z) = \frac{1}{4\pi}\iint_S (\Delta\bar{I})\frac{\partial}{\partial z}\left(\frac{1}{r}\right) dx'\,dy' , \quad \ldots \quad (14)$$

where

$$r^2 = (x - x')^2 + (1 - M^2)\,\{(y - y')^2 + z^2\}.$$

It follows from equations (13) and (14) that

$$\bar{I}(x, y, z) = -\frac{U^2 z(1 - M^2)}{8\pi}\iint_S \frac{\bar{l}(x', y')\,dx'\,dy'}{[(x - x')^2 + (1 - M^2)\,\{(y - y')^2 + z^2\}]^{3/2}} . \quad \ldots \quad (15)$$

The geometry of the wing and its motion are brought into the problem by specifying the component of velocity w in the last of the equations (5). On writing

$$w = \mathscr{R}\left\{\bar{w}\exp\left\{i\omega\left(t + \frac{x}{U}\frac{M^2}{1 - M^2}\right)\right\}\right\} \quad \ldots \quad (16)$$

similarly to equation (8) with the value of λ from equation (9), differentiation along a streamline gives

$$\left(\frac{\partial}{\partial t} + U\frac{\partial}{\partial x}\right) w = \mathscr{R}\left\{\left[U\frac{\partial\bar{w}}{\partial x} + i\omega\bar{w}\left(1 + \frac{M^2}{1 - M^2}\right)\right]\exp\left\{i\omega\left(t + \frac{x}{U}\frac{M^2}{1 - M^2}\right)\right\}\right\} .$$

By cancelling the common exponential factor, the equation (5) becomes

$$U\frac{\partial\bar{w}}{\partial x} + \frac{i\omega\bar{w}}{1 - M^2} + \frac{\partial\bar{I}}{\partial z} = 0 . \quad \ldots \quad (17)$$

This differential equation for $\bar{w}$ may be written as

$$\frac{\partial}{\partial x}\left[\bar{w}\exp\left\{\frac{i\omega x}{U(1 - M^2)}\right\}\right] + \frac{1}{U}\frac{\partial\bar{I}}{\partial z}\exp\left\{\frac{i\omega x}{U(1 - M^2)}\right\} = 0 .$$

By integrating along the lines $y =$ constant, $z = 0$,

$$\bar{w} = -\frac{1}{U}\int_{-\infty}^{x}\frac{\partial\bar{I}}{\partial z}(x_0, y, 0)\exp\left\{\frac{i\omega\,(x_0 - x)}{U(1 - M^2)}\right\} dx_0 . \quad \ldots \quad (18)$$

From equations (15) and (18),

$$\bar{w}(x, y) = \frac{U(1 - M^2)}{8\pi}\int_{-\infty}^{x}\left\{\iint_S \frac{l(x', y')\,dx'\,dy'}{[(x_0 - x')^2 + (1 - M^2)(y - y')^2]^{3/2}}\right\}\exp\left\{\frac{i\omega(x_0 - x)}{U(1 - M^2)}\right\}dx_0\,. \quad (19)$$

So far the only restriction on frequency is the approximation that $\omega\bar{c}M/U(1 - M^2)$ is small. This implies that equation (19) is not valid for any frequency at transonic speeds, is valid to the first order in frequency at sub-critical Mach numbers, and is valid for all frequencies in incompressible flow.

3. *Steady Motion.*—Before proceeding with the theory of pitching oscillations, it will be helpful to consider briefly the treatment of problems in steady flow. On substituting $\omega = 0$ and $M = 0$, the basic equation (19) reduces to

$$w(x, y) = \frac{U}{8\pi}\iint_S l(x', y')\int_{-\infty}^{x}\frac{dx_0}{[(x_0 - x')^2 + (y - y')^2]^{3/2}}\,dx'\,dy'$$

or

$$\alpha(x, y) = -\frac{w}{U} = -\frac{1}{8\pi}\iint_S \frac{l(x', y')}{(y - y')^2}\left[1 + \frac{x - x'}{\sqrt{\{(x - x')^2 + (y - y')^2\}}}\right]dx'\,dy'\,, \quad \ldots \quad (20)$$

which corresponds to equation (15) of Ref. 1. At each section y' the chordwise loading is expressed as a series, which includes as many terms as there are boundary conditions at each pivotal station. In the present treatment the number of terms is restricted to two, so that

$$l(x', y') = \frac{8s\gamma(y')}{\pi c(y')}\cot\tfrac{1}{2}\phi + \frac{32s\mu(y')}{\pi c(y')}(\cot\tfrac{1}{2}\phi - 2\sin\phi)\,, \quad \ldots \quad (21)$$

where s is the semi-span of the wing,

$$x' = x_l'(y') + \tfrac{1}{2}c(y')(1 - \cos\phi)$$

and $x' = x_l'(y')$ is the equation of the leading edge,

so that $\phi = 0$ and $\phi = \pi$ correspond to the leading and trailing edges. It follows that

$$\alpha(x, y) = -\frac{1}{2\pi}\int_{-1}^{1}\frac{(\gamma.i + \mu.j)\,d\eta'}{(\eta - \eta')^2}\,, \quad \ldots \quad (22)$$

where the spanwise variables η, $\eta' = y/s$, y'/s, and the influence functions i and j are determined by the chordwise integrations

$$\left.\begin{aligned} i(X, Y) &= \frac{1}{\pi}\int_0^{\pi}\cot\tfrac{1}{2}\phi\left[1 + \frac{X - \frac{1}{2}(1 - \cos\phi)}{\sqrt{[\{X - \frac{1}{2}(1 - \cos\phi)\}^2 + Y^2]}}\right]\sin\phi\,d\phi \\ j(X, Y) &= \frac{4}{\pi}\int_0^{\pi}(\cot\tfrac{1}{2}\phi - 2\sin\phi)\left[1 + \frac{X - \frac{1}{2}(1 - \cos\phi)}{\sqrt{[\{X - \frac{1}{2}(1 - \cos\phi)\}^2 + Y^2]}}\right]\sin\phi\,d\phi \end{aligned}\right\}\,, \quad (23)$$

with $$\left.\begin{aligned} X &= (x - x_l')/c(y') \\ Y &= (y - y')/c(y') \end{aligned}\right\} .$$

The spanwise integration of equation (22) is achieved by the technique of interpolation used in Multhopp's treatment of the 'lifting-line' theory. This is described in Ref. 1, section 5.1. By specifying an odd integer m, the unknown functions $\gamma(y')$, $\mu(y')$ are represented by polynomials in terms of their values at the m pivotal stations

$$y_n' = s \sin \frac{n\pi}{m+1} \left[n = 0, \pm 1, \pm 2, \ldots . \pm \tfrac{1}{2}(m-1)\right] .$$

It is then possible to express $\alpha(x, y)$ at the pivotal station $y = y_\nu$ as a positive contribution from the polynomial term belonging to the station itself and negative or zero contributions from the other terms. Thus

$$\alpha_\nu(x) = b_{\nu\nu}(\gamma i + \mu j)_\nu - \sum_{-\frac{1}{2}(m-1)}^{\frac{1}{2}(m-1)}{}' \, b_{\nu n}(\gamma i + \mu j)_n , \qquad (24)$$

where

$$b_{\nu\nu} = \frac{m+1}{4 \cos \dfrac{\nu\pi}{m+1}}$$

$$\begin{aligned} b_{\nu n} &= \frac{\cos \dfrac{n\pi}{m+1}}{(m+1)\left[\sin \dfrac{n\pi}{m+1} - \sin \dfrac{\nu\pi}{m+1}\right]^2} & |\nu - n| &= 1, 3, 5, \ldots \\ &= 0 & |\nu - n| &= 2, 4, 6, \ldots \end{aligned}$$

and Σ' denotes that the value $n = \nu$ is not included in the summation.

There are however logarithmic singularities in the second derivatives of i and j with respect to Y. As shown in Ref. 1, equation (53), near the inducing section $y = y'$, $i(X, Y)$ can only be developed into a series beginning with

$$i(X, Y) = i(X, 0) + K_1(i) Y^2 \log |Y| + \ldots\ldots , \qquad (25)$$

where

$$i(X, 0) = \frac{2}{\pi}\left[\cos^{-1}(1 - 2X) + 2\sqrt{\{X(1 - X)\}}\right]$$

and $$K_1(i) = 1/\pi X^{3/2} \sqrt{(1 - X)} .$$

Therefore the polynomial representation implicit in equation (24) is not accurate enough. By the treatment given in Ref. 1, section 5.2, a correction

$$\Delta\alpha_\nu(x) = \frac{92}{225\pi} \{\gamma_\nu K_1(i) + \mu_\nu K_1(j)\} \left(\frac{s}{c_\nu}\right)^2 (\eta_{\nu+1} - \eta_{\nu-1}) \qquad (26)$$

is obtained. When this correction† is added to equation (24),

$$\alpha_\nu(x) = b_{\nu\nu}[\overline{i_{\nu\nu}}\, \gamma_\nu + \overline{j_{\nu\nu}}\, \mu_\nu] - \sum_{-\frac{1}{2}(m-1)}^{\frac{1}{2}(m-1)}{}' \, b_{\nu n}(i_{\nu n}\, \gamma_n + j_{\nu n}\, \mu_n) , \qquad (27)$$

† An improved treatment of the logarithmic singularity has been given by Mangler and Spencer[13] whose corrections supersede equation (26).

where

$$\overline{i_{\nu\nu}} = \frac{2}{\pi}\left[\cos^{-1}(1-2X) + 2\sqrt{\{X(1-X)\}}\right] + \frac{1}{\pi X^{3/2}\sqrt{(1-X)}} \cdot F_\nu$$

$$\overline{j_{\nu\nu}} = \frac{32}{\pi} X^{1/2}(1-X)^{3/2} + \frac{4(1+4X-8X^2)}{\pi X^{3/2}\sqrt{(1-X)}} \cdot F_\nu$$

with

$$F_\nu = \frac{368}{225\pi}\,\frac{1}{m+1}\cos\frac{\nu\pi}{m+1}\,(\eta_{\nu+1} - \eta_{\nu-1})\left(\frac{s}{c_\nu}\right)^2 .$$

A further complication arises at the kinked central section of swept wings. On substituting the loading $l(x', y')$ from equation (21), a logarithmic singularity in downwash would arise in the integral (20), wherever $\partial\phi/\partial y'$ is discontinuous. Multhopp overcomes this difficulty at a kinked section by calculating the downwash of an 'interpolated wing' (Ref. 1, section 5.3). This amounts to a simple change in the geometry of the wing at the section $y' = y_0' = 0$. The local values $x_{0l}' = 0$ and $c(y_0') = c_r$, root chord, are replaced by

$$\left.\begin{aligned} x_{0l}' &= \tfrac{1}{6}x_{1l}' \\ c(y_0') &= c_r - \tfrac{1}{6}\{c_r - c(y_1')\} \end{aligned}\right\} \qquad (28)$$

in terms of the neighbouring pivotal station $n = 1$. The calculated loads at the central section from equation (21) must be referred to the actual geometrical section in such a way that the local lift and position of centre of pressure are those determined for the 'interpolated wing.'

The boundary conditions (27) are satisfied at two points on each pivotal station. For the reasons put forward in Ref. 1, section 3, the chordwise positions are chosen such that $\phi = 4\pi/5$ and $2\pi/5$. In the notation of equation (21) these correspond to chordwise positions

$$\left.\begin{aligned} x_\nu' &= x_{\nu l} + 0\cdot9045c_\nu \\ x_\nu'' &= x_{\nu l} + 0\cdot3455c_\nu \end{aligned}\right\}, \qquad (29)$$

where the subscript ν indicates that $y' = y_\nu' = s\sin\{\nu\pi/(m+1)\}$.

From the two conditions at each pivotal station the unknowns γ_ν and μ_ν are separated by elimination. Thus the $2m$ equations (27) are expressed in the most convenient form for solution:

$$\left.\begin{aligned} \gamma_\nu = a_{\nu\nu}(l_\nu'\alpha_\nu' - l_\nu''\alpha_\nu'') &+ \sum_{-\frac{1}{2}(m-1)}^{\frac{1}{2}(m-1)}{}' a_{\nu n}(l_\nu' i_{\nu n}' - l_\nu'' i_{\nu n}'')\gamma_n \\ &+ \sum_{-\frac{1}{2}(m-1)}^{\frac{1}{2}(m-1)}{}' a_{\nu n}(l_\nu' j_{\nu n}' - l_\nu'' j_{\nu n}'')\mu_n \\ \mu_\nu = a_{\nu\nu}(m_\nu''\alpha_\nu'' - m_\nu'\alpha_\nu') &+ \sum_{-\frac{1}{2}(m-1)}^{\frac{1}{2}(m-1)}{}' a_{\nu n}(m_\nu'' i_{\nu n}'' - m_\nu' i_{\nu n}')\gamma_n \\ &+ \sum_{-\frac{1}{2}(m-1)}^{\frac{1}{2}(m-1)}{}' a_{\nu n}(m_\nu'' j_{\nu n}'' - m_\nu' j_{\nu n}')\mu_n \end{aligned}\right\} \qquad (30)$$

where

$$\frac{l_\nu'}{\overline{j_{\nu\nu}''}} = \frac{l_\nu''}{\overline{j_{\nu\nu}'}} = \frac{m_\nu'}{\overline{i_{\nu\nu}''}} = \frac{m_\nu''}{\overline{i_{\nu\nu}'}} = \frac{1}{\overline{i_{\nu\nu}'}\,\overline{j_{\nu\nu}''} - \overline{i_{\nu\nu}''}\,\overline{j_{\nu\nu}'}},$$

$$a_{\nu\nu} = a_{\nu n}/b_{\nu n} = 1/b_{\nu\nu}$$

and the single stroke ′ and the double stroke ″ denote respective substitutions $x = x_\nu'$ and $x = x_\nu''$ from equation (29). The quantities $a_{\nu\nu}$ and $a_{\nu n} = a_{n\nu}$ are independent of plan-form and given in Ref. 1, Tables 1 to 7 for the particular values of $m = 3, 5, 7, 11, 15, 23, 31$. Numerical formulae for $\bar{i}_{\nu\nu}'$, $\bar{j}_{\nu\nu}'$, $\bar{i}_{\nu\nu}''$, $\bar{j}_{\nu\nu}''$ according to equations (27) are found in Ref. 1, equations (86). The influence functions i and j from equations (23) are given graphically in terms of X and Y in Ref. 1, Figs. 1 to 6. With these aids equations (30) may be evaluated economically. Since $a_{\nu n} = 0$ for $|\nu - n| = 2, 4, 6, \ldots$, the equations express each unknown (n odd) directly in terms of all the unknowns of the other set (n even) and *vice versa*. An iterative solution for the $2m$ unknowns γ_n and μ_n is therefore possible by considering separately the sets of equations with n even and with n odd.

The aerodynamic forces and moments then follow from Ref. 1, section 7, where the coefficients are determined from the chordwise loadings in equation (21) by integrating the polynomials assumed in the calculation of downwash. The lift and pitching moment about the local quarter chord per unit span are:

$$dL/dy = 2\rho U^2 s\gamma$$

$$d\mathcal{M}/dy = 2\rho U^2 sc\mu .$$

Hence

$$C_L = \frac{\pi A}{m+1} \sum_{-\frac{1}{2}(m-1)}^{\frac{1}{2}(m-1)} \gamma_n \cos \frac{n\pi}{m+1} \qquad (31)$$

$$C_l = \frac{\pi A}{4(m+1)} \sum_{-\frac{1}{2}(m-1)}^{\frac{1}{2}(m-1)} \gamma_n \sin \frac{2n\pi}{m+1} . \qquad (32)$$

The position of the local centre of pressure measured as a fraction of the local chord from the leading edge of any section is

$$X_{\text{a.c.}} = \frac{1}{4} - \frac{\mu_n}{\gamma_n} \, (n \neq 0) .$$

In the particular case of the central section, $n = 0$, this formula is modified to take account of the 'interpolated wing,' and

$$X_{\text{a.c.}} = \frac{1}{c_r} \left\{ x_{0l} + \left(\frac{1}{4} - \frac{\mu_0}{\gamma_0} \right) c_0 \right\} , \qquad (33)$$

where x_{0l} and c_0 are determined as in equation (28). The coefficient of pitching moment about the y-axis is

$$C_m = \frac{\pi A^2}{2(m+1)} \sum_{-\frac{1}{2}(m-1)}^{\frac{1}{2}(m-1)} \left\{ \mu_n \frac{c_n}{s} - \gamma_n \left(\frac{x_{nl}}{s} + \frac{1}{4}\frac{c_n}{s} \right) \right\} \cos \frac{n\pi}{m+1} . \qquad (34)$$

The results are given here quite generally for asymmetrical distributions. In practice it is usual to have either symmetry, $\gamma_n = \gamma_{-n}$ and $\mu_n = \mu_{-n}$, or antisymmetry, $\gamma_n = -\gamma_{-n}$ and $\mu_n = -\mu_{-n}$; the equations (30), and formulae (31), (32), (34) then simplify.

Considerable difficulties have been experienced in reading the charts (Ref. 1, Figs. 1 to 6) for the influence functions i and j; and a complete tabulation of both functions was clearly desirable. This has been carried out by the staff of the Mathematics Division of the N.P.L.[11] (Curtis, 1952). The tables use polar co-ordinates (R, ψ), such that

$$\left. \begin{aligned} R \cos \psi &= 2X - 1 \\ R \sin \psi &= 2Y \end{aligned} \right\} . \qquad (35)$$

In the area $R \leqslant 2$, i and j are tabulated for $\psi = 0$ deg (1 deg) 180 deg, $R = 0{\cdot}20(0{\cdot}05)2{\cdot}00$. In the area $R \geqslant 2$, i and j are tabulated for $\psi = 0$ deg (1 deg) 180 deg, $1/R = 0{\cdot}00(0{\cdot}05)0{\cdot}50$. The use of these tables necessitates some alterations to the computational scheme set out in Ref. 1, Tables 14 to 17. But basically the calculation is unaffected and results in sets of equations (30).

4. *Limiting Frequency*.—In section 2 it was shown that, if the square of the quantity $\omega\bar{c}M/U(1 - M^2)$ is negligible, it is possible to write the oscillating load and upwash at the wing as

$$\left.\begin{aligned} \Delta p/\tfrac{1}{2}\rho U^2 = l(x', y', t) &= \mathscr{R}\left\{\bar{l}(x', y') \exp[i\omega\{t + x'M^2/U(1 - M^2)\}]\right\} \\ w(x, y, t) &= \mathscr{R}\left\{\bar{w}(x, y) \exp[i\omega\{t + xM^2/U(1 - M^2)\}]\right\} \end{aligned}\right\} \quad \ldots \quad (36)$$

and to obtain the integral relation between their complex amplitudes

$$\bar{w}(x,y) = \frac{U(1-M^2)}{8\pi}\int_{-\infty}^{x}\left\{\iint_S \frac{\bar{l}(x', y')\, dx'\, dy'}{[(x_0-x')^2+(1-M^2)(y-y')^2]^{3/2}}\right\}\exp\{i\omega(x_0-x)/U(1-M^2)\}dx_0 \,. \quad (37)$$

Equations (36) and (37) summarize equations (8), (9), (12), (16) and (19) of section 2.

The treatment of equation (37), when ω is small, is discussed in Appendix I. The integrand may be expanded to the first power in ω by writing

$$\exp\{i\omega(x_0 - x)/U(1 - M^2)\} = 1 - \frac{i\omega(x - x_0)}{U(1 - M^2)} \,. \quad \ldots \quad \ldots \quad (38)$$

It is shown in Appendix I that this approximation neglects a term of order $\omega^2 \log \omega$ in $\bar{w}(x, y)$. For slow oscillations equation (37) is conveniently split into two parts corresponding to the separate terms of equation (38) to give

$$\bar{w} = \bar{w}_1 + i\bar{w}_2, \quad \ldots \quad \ldots \quad \ldots \quad \ldots \quad \ldots \quad \ldots \quad \ldots \quad \ldots \quad (39)$$

where

$$\bar{w}_1(x, y) = \frac{U(1 - M^2)}{8\pi}\int_{-\infty}^{x}\left\{\iint_S \frac{\bar{l}(x', y')\, dx'\, dy'}{[(x_0 - x')^2 + (1 - M^2)(y - y')^2]^{3/2}}\right\} dx_0$$

$$-\bar{w}_2(x, y) = \frac{\omega}{8\pi}\int_{-\infty}^{x}(x - x_0)\left\{\iint_S \frac{\bar{l}(x', y')\, dx'\, dy'}{[(x_0 - x')^2 + (1 - M^2)(y - y')^2]^{3/2}}\right\} dx_0 \,\ldots$$

Like $\bar{l}$, both $\bar{w}_1$ and $\bar{w}_2$ are complex quantities. From the simple integration

$$\int_{-\infty}^{x}\frac{dx_0}{[(x_0 - x')^2 + (1 - M^2)(y - y')^2]^{3/2}}$$

$$= \frac{1}{(1 - M^2)(y - y')^2}\left[1 + \frac{x - x'}{\sqrt{\{(x - x')^2 + (1 - M^2)(y - y')^2\}}}\right]$$

the first component of $\bar{w}$ comes to

$$\bar{w}_1(x, y) = \frac{U}{8\pi}\iint_S \frac{\bar{l}(x', y')}{(y - y')^2}\left[1 + \frac{x - x'}{\sqrt{\{(x - x')^2 + (1 - M^2)(y - y')^2\}}}\right] dx'\, dy', \quad \ldots \quad (40)$$

which is formally identical to the integral for the steady downwash in equation (20). The second component $\bar{w}_2$ requires an integration by parts

$$\int_{-\infty}^{x} \frac{(x - x_0)\, dx_0}{[(x_0 - x')^2 + (1 - M^2)(y - y')^2]^{3/2}}$$

$$= \left[\frac{x - x_0}{(1 - M^2)(y - y')^2}\left\{1 + \frac{x_0 - x'}{\sqrt{\{(x_0 - x')^2 + (1 - M^2)(y - y')^2\}}}\right\}\right]_{x_0=-\infty}^{x_0=x}$$

$$+ \frac{1}{(1 - M^2)(y - y')^2}\int_{-\infty}^{x}\left\{1 + \frac{x_0 - x'}{\sqrt{\{(x_0 - x')^2 + (1 - M^2)(y - y')^2\}}}\right\} dx_0 .$$

The first integral vanishes at both limits. Hence

$$- \bar{w}_2(x, y) = \frac{\omega}{8\pi(1 - M^2)} \iint_S \frac{\bar{l}(x', y')}{(y - y')^2}$$

$$\left[\int_{-\infty}^{x}\left\{1 + \frac{x_0 - x'}{\sqrt{\{(x_0 - x')^2 + (1 - M^2)(y - y')^2\}}}\right\} dx_0\right] dx'\, dy' \quad .. \qquad (41)$$

For the practical computation of these integrals (40) and (41), the chordwise load distribution is expressed as a linear combination of the distributions that occur most prominently in two-dimensional steady theory. Following equation (21),

$$\bar{l}(x', y') = \frac{8s\bar{\gamma}(y')}{\pi c(y')} \cot \tfrac{1}{2}\phi + \frac{32s\bar{\mu}(y')}{\pi c(y')} (\cot \tfrac{1}{2}\phi - 2 \sin \phi) . \quad .. \quad .. \quad .. \qquad (42)$$

Then, precisely as in steady motion (equations (22) and (23)), at the section $y = s\eta$,

$$\frac{\bar{w}_1(x)}{U} = \frac{1}{2\pi}\int_{-1}^{1} \frac{\bar{\gamma}(\eta')i(\eta, \eta') + \bar{\mu}(\eta')j(\eta, \eta')}{(\eta - \eta')^2}\, d\eta' \quad .. \quad .. \quad .. \quad .. \qquad (43)$$

with

$$\left.\begin{aligned} i(X, Y) &= 1 + \frac{1}{\pi}\int_0^{\pi} \frac{2X - 1 + \cos\phi}{\sqrt{\{(2X - 1 + \cos\phi)^2 + 4Y^2\}}} (1 + \cos\phi)\, d\phi \\ j(X, Y) &= \frac{4}{\pi}\int_0^{\pi} \frac{2X - 1 + \cos\phi}{\sqrt{\{(2X - 1 + \cos\phi)^2 + 4Y^2\}}} (2\cos^2\phi + \cos\phi - 1)\, d\phi \end{aligned}\right\} \quad .. \qquad (44)$$

where

$$X = (x - x_l')/c(y')$$
$$Y = (1 - M^2)^{1/2}(y - y')/c(y').$$

On substituting $X_0 = (x_0 - x_l')/c(y')$, the integral (41) at the section $y = s\eta$ becomes

$$-\frac{\bar{w}_2(x)}{U} = \frac{\omega\bar{c}}{U(1 - M^2)}\,\frac{1}{2\pi}\int_{-1}^{1} \frac{c(\eta')}{\bar{c}}\,\frac{\bar{\gamma}(\eta')\, ii(\eta, \eta') + \bar{\mu}(\eta')\, jj(\eta, \eta')}{(\eta - \eta')^2}\, d\eta' \quad .. \quad .. \qquad (45)$$

with

$$
\left.\begin{aligned}
ii(X, Y) &= \int_{-\infty}^{X} i(X_0, Y)\, dX_0 \\
jj(X, Y) &= \int_{-\infty}^{X} j(X_0, Y)\, dX_0
\end{aligned}\right\} \quad \ldots \quad (46)
$$

As explained in section 3, the steady influence functions i and j are conveniently tabulated in polar co-ordinates (R, ψ), such that

$$
\left.\begin{aligned}
R \cos \psi &= 2X - 1 \\
R \sin \psi &= 2Y
\end{aligned}\right\} .
$$

Complete tables of all the influence functions i, j, ii and jj from equations (44) and (46) are available from the N.P.L. (Ref. 11).

The numerical treatment of the integrals (43) and (45) is discussed briefly in section 3 and given in detail in Ref. 1. From equations (22) and (27), the integrals for $\bar{w}$ at $y = s\eta_\nu = s \sin \{\nu\pi/(m + 1)\}$ reduce to summations

$$
-\frac{\bar{w}_1(x)}{U} = b_{\nu\nu}[\overline{i_{\nu\nu}}\bar{\gamma}_\nu + \bar{j}_{\nu\nu}\bar{\mu}_\nu] - \sum_{-\frac{1}{2}(m-1)}^{\frac{1}{2}(m-1)}{}' b_{\nu n}(i_{\nu n}\bar{\gamma}_n + j_{\nu n}\bar{\mu}_n) \quad \ldots \quad (47)
$$

$$
\frac{U(1 - M^2)}{\omega\bar{c}} \frac{\bar{w}_2(x)}{U} = b_{\nu\nu} \frac{c_\nu}{\bar{c}} [\overline{ii_{\nu\nu}}\, \bar{\gamma}_\nu + \overline{jj_{\nu\nu}}\bar{\mu}_\nu] - \sum_{-\frac{1}{2}(m-1)}^{\frac{1}{2}(m-1)}{}' b_{\nu n} \frac{c_n}{\bar{c}} (ii_{n\nu}\bar{\gamma}_n + jj_{\nu n}\bar{\mu}_n) \quad \ldots \quad (48)
$$

with

$$
\left.\begin{aligned}
\overline{ii_{\nu\nu}} &= ii(X, 0) + K_1(ii)\, F_\nu \\
\overline{jj_{\nu\nu}} &= jj(X, 0) + K_1(jj)\, F_\nu
\end{aligned}\right\} \quad \ldots \quad (49)
$$

where

$$
F_\nu = \frac{368}{225\pi} \frac{1}{m + 1} \cos \frac{\nu\pi}{m + 1} (\eta_{\nu+1} - \eta_{\nu-1}) \left(\frac{s}{c_\nu}\right)^2 (1 - M^2),
$$

and K_1 is defined by an equation similar to (25). By the methods used in section 4, of Ref. 1, equation (46) gives

$$
\begin{aligned}
ii(X, 0) &= \int_{-\infty}^{X} i(X_0, 0)\, dX_0 = \int_{0}^{X} i(X_0, 0)\, dX_0 \\
&= \frac{2}{\pi} \int_{0}^{X} [\cos^{-1}(1 - 2X_0) + 2\sqrt{\{X_0(1 - X_0)\}}]\, dX_0 \\
&= \frac{2}{\pi} [(X - \tfrac{1}{4}) \cos^{-1}(1 - 2X) + (\tfrac{1}{2} + X) \sqrt{\{X(1 - X)\}}] \quad \ldots \quad (50)
\end{aligned}
$$

$$
\begin{aligned}
jj(X, 0) &= \int_{-\infty}^{X} j(X_0, 0)\, dX_0 = \frac{32}{\pi} \int_{0}^{X} X_0^{1/2} (1 - X_0)^{3/2}\, dX_0 \\
&= \frac{2}{\pi} \cos^{-1}(1 - 2X) + \frac{4}{3\pi} (4X - 1)(3 - 2X)\sqrt{\{X(1 - X)\}} . \quad \ldots \quad (51)
\end{aligned}
$$

Furthermore the coefficient K_1 in the expansion

$$ii(X, Y) = ii(X, 0) + K_1(ii) Y^2 \log |Y| + \dots$$

is given by equations similar to (49) and (54) of Ref. 1. Thus

$$\left.\begin{aligned} K_1(ii) &= -\frac{1}{2}\frac{\partial^2}{\partial X^2}[ii(X, 0)] = -\frac{2}{\pi}\sqrt{\left\{\frac{1-X}{X}\right\}} \\ K_1(jj) &= -\frac{1}{2}\frac{\partial^2}{\partial X^2}[jj(X, 0)] = \frac{8}{\pi}\sqrt{\left\{\frac{1-X}{X}\right\}}(4X-1) \end{aligned}\right\} \quad \dots \quad \dots \quad (52)$$

It remains to substitute the values $y = s\eta_\nu = s \sin\{\nu\pi/(m+1)\}$ and $x = x_\nu'$, $x = x_\nu''$ from equation (29) to obtain $\bar{w}_1$ and $\bar{w}_2$ at the chordwise solving positions $0 \cdot 9045c$, $0 \cdot 3455c$ at the pivotal stations ν. The inducing station is

$$y' = s\eta_n = s \sin \frac{n\pi}{m+1}.$$

Then from equation (44),

$$\left.\begin{aligned} X_{\nu n}' &= (x_\nu' - x_{nl})/c_n \,;\; X_{\nu n}'' = (x_\nu'' - x_{nl})/c_n \\ |Y_{\nu n}'| &= |Y_{\nu n}''| = s|\eta_\nu - \eta_n|(1 - M^2)^{1/2}/c_n \end{aligned}\right\} \quad \dots \quad \dots \quad \dots \quad \dots \quad (53)$$

In the special case $n = \nu$, $X_{\nu\nu}' = 0 \cdot 9045$, $X_{\nu\nu}'' = 0 \cdot 3455$. At these positions $\overline{i_{\nu\nu}}$ and $\overline{j_{\nu\nu}}$ are calculated in Ref. 1, equation (86), and $\overline{ii_{\nu\nu}}$ and $\overline{jj_{\nu\nu}}$ may be evaluated from equations (49), (50), (51) and (52) as follows† :

$$\left.\begin{aligned}
\text{at } 0 \cdot 9045c, \quad \overline{i_{\nu\nu}'} &= 1 \cdot 9742 + 0 \cdot 6234 \left(\frac{s\beta}{c_\nu}\right)^2 \frac{\eta_{\nu+1} - \eta_{\nu-1}}{m+1} \cos \frac{\nu\pi}{m+1} \\
\overline{j_{\nu\nu}'} &= 0 \cdot 2859 - 4 \cdot 8053 \left(\frac{s\beta}{c_\nu}\right)^2 \frac{\eta_{\nu+1} - \eta_{\nu-1}}{m+1} \cos \frac{\nu\pi}{m+1} \\
\overline{ii_{\nu\nu}'} &= 1 \cdot 3100 - 0 \cdot 1077 \left(\frac{s\beta}{c_\nu}\right)^2 \frac{\eta_{\nu+1} - \eta_{\nu-1}}{m+1} \cos \frac{\nu\pi}{m+1} \\
\overline{jj_{\nu\nu}'} &= 1 \cdot 9889 + 1 \cdot 1281 \left(\frac{s\beta}{c_\nu}\right)^2 \frac{\eta_{\nu+1} - \eta_{\nu-1}}{m+1} \cos \frac{\nu\pi}{m+1} \\
\text{at } 0 \cdot 3455c, \quad \overline{i_{\nu\nu}''} &= 1 \cdot 4055 + 1 \cdot 0087 \left(\frac{s\beta}{c_\nu}\right)^2 \frac{\eta_{\nu+1} - \eta_{\nu-1}}{m+1} \cos \frac{\nu\pi}{m+1} \\
\overline{j_{\nu\nu}''} &= 3 \cdot 1702 + 5 \cdot 7577 \left(\frac{s\beta}{c_\nu}\right)^2 \frac{\eta_{\nu+1} - \eta_{\nu-1}}{m+1} \cos \frac{\nu\pi}{m+1} \\
\overline{ii_{\nu\nu}''} &= 0 \cdot 3323_5 - 0 \cdot 4563 \left(\frac{s\beta}{c_\nu}\right)^2 \frac{\eta_{\nu+1} - \eta_{\nu-1}}{m+1} \cos \frac{\nu\pi}{m+1} \\
\overline{jj_{\nu\nu}''} &= 0 \cdot 9780 + 0 \cdot 6972 \left(\frac{s\beta}{c_\nu}\right)^2 \frac{\eta_{\nu+1} - \eta_{\nu-1}}{m+1} \cos \frac{\nu\pi}{m+1}
\end{aligned}\right\} \quad \dots \quad \dots \quad (54)$$

where $\dfrac{\eta_{\nu+1} - \eta_{\nu-1}}{m+1} \cos \dfrac{\nu\pi}{m+1}$ is tabulated in Ref. 1 (Tables 1 to 7), and $\beta = \sqrt{(1 - M^2)}$.

† Improved formulae to replace equations (54) may be deduced from Ref. 13 ; these are given in the special cases $m = 7$, $m = 11$ and $m = 15$ at the end of Appendix II.

To summarize, from equations (37), (42), (47) and (48), the angle of upwash at the pivotal station ν is represented by

$$\frac{\bar{w}(x)}{U} = \frac{\bar{w}_1(x)}{U} + i\,\frac{\bar{w}_2(x)}{U}$$

$$= -\,b_{\nu\nu}\left[\left(\overline{i_{\nu\nu}} - \frac{i\omega c_\nu \overline{ii_{\nu\nu}}}{U(1-M^2)}\right)\bar{\gamma}_\nu + \left(\overline{j_{\nu\nu}} - \frac{i\omega c_\nu \overline{jj_{\nu\nu}}}{U(1-M^2)}\right)\bar{\mu}_\nu\right.$$

$$\left. -\sum_{-\frac{1}{2}(m-1)}^{\frac{1}{2}(m-1)}{}' a_{\nu n}\left\{\left(i_{\nu n} - \frac{i\omega c_n ii_{\nu n}}{U(1-M^2)}\right)\bar{\gamma}_n + \left(j_{\nu n} - \frac{i\omega c_n jj_{\nu n}}{U(1-M^2)}\right)\bar{\mu}_n\right\}\right], \quad (55)$$

where from equation (24)

$$\left.\begin{aligned} a_{\nu n} = b_{\nu n}/b_{\nu\nu} &= \frac{4\cos\dfrac{\nu\pi}{m+1}\cos\dfrac{n\pi}{m+1}}{(m+1)^2\,(\eta_\nu - \eta_n)^2} \qquad &|\nu - n| = 1, 3, 5, \ldots \\ &= 0 &|\nu - n| = 2, 4, 6, \ldots \end{aligned}\right\}.$$

Values of $a_{\nu n}$ are found in Tables 1 to 7 of Ref. 1 for $m = 3, 5, 7, 11, 15, 23, 31$ to suit all practical requirements. The values of $\overline{i_{\nu\nu}}$, $\overline{j_{\nu\nu}}$, $\overline{ii_{\nu\nu}}$, $\overline{jj_{\nu\nu}}$ for the important positions

$$\left.\begin{aligned} x = x_\nu' &= x_{\nu l} + 0\cdot 9045c_\nu \\ x = x_\nu'' &= x_{\nu l} + 0\cdot 3455c_\nu \end{aligned}\right\} \quad \ldots \quad (56)$$

are given in equations (54). Tables of the general influence functions i, j, ii, jj are compiled in Ref. 11, as described in section 3 (equation (35)), X and Y being given in equation (53).

5. *Pitching Oscillations.*—Let an uncambered thin wing oscillate about a pitching axis $x = x_0$. At an incidence α the wing surface is given by

$$z = -\,\alpha(x - x_0).$$

If the oscillation is of amplitude Q and frequency ω, the surface becomes

$$\begin{aligned} z &= -\,Q(x - x_0)\cos\omega t \\ &= \mathscr{R}\{-\,Q(x - x_0)\exp(i\omega t)\}\,. \end{aligned} \quad \ldots \quad (57)$$

Hence

$$\left.\begin{aligned} \alpha &= \mathscr{R}\{Q\exp(i\omega t)\} \\ \frac{\partial\alpha}{\partial t} &= \dot{\theta} = \mathscr{R}\{i\omega Q\exp(i\omega t)\} \end{aligned}\right\} \quad \ldots \quad (58)$$

The upward component of velocity at the surface must satisfy

$$\begin{aligned} w &= \frac{\partial z}{\partial t} + U\frac{\partial z}{\partial x} \\ &= \mathscr{R}\Big\{-\,\{QU + i\omega Q(x - x_0)\}\exp(i\omega t)\Big\}\,. \end{aligned} \quad \ldots \quad (59)$$

By combining equations (16) and (59),

$$\frac{\bar{w}}{U} = -Q\left(1 + \frac{i\omega(x - x_0)}{U}\right)\exp\left\{-\frac{i\omega x}{U}\frac{M^2}{1 - M^2}\right\}$$

$$= -Q\left(1 + \frac{i\omega x}{U}\frac{1 - 2M^2}{1 - M^2} - \frac{i\omega x_0}{U}\right), \qquad (60)$$

when for slow oscillations only those terms independent of or linear in $\omega x/U$ are retained.

From equations (36) and (42), the oscillating load on the wing is

$$\frac{\Delta p}{\frac{1}{2}\rho U^2} = \mathscr{R}\left\{\bar{l}\exp[i\omega\{t + xM^2/U(1 - M^2)\}]\right\}$$

with

$$\bar{l}(x, y) = \frac{8s\bar{\gamma}(y)}{\pi c(y)}\cot\tfrac{1}{2}\phi + \frac{32s\bar{\mu}(y)}{\pi c(y)}(\cot\tfrac{1}{2}\phi - 2\sin\phi), \qquad (61)$$

where

$$x = x_l(y) + \tfrac{1}{2}c(y)(1 - \cos\phi).$$

When the boundary condition (60) at the plan-form is combined with equation (55),

$$\frac{Q}{b_{\nu\nu}}\left(1 + \frac{i\omega x}{U}\frac{1 - 2M^2}{1 - M^2} - \frac{i\omega x_0}{U}\right) = \left\{\bar{i}_{\nu\nu} - \frac{i\omega c_\nu \overline{ii}_{\nu\nu}}{U(1 - M^2)}\right\}\bar{\gamma}_\nu + \left\{\bar{j}_{\nu\nu} - \frac{i\omega c_\nu \overline{jj}_{\nu\nu}}{U(1 - M^2)}\right\}\bar{\mu}_\nu$$

$$- \sum_{-\frac{1}{2}(m-1)}^{\frac{1}{2}(m-1)}{}' a_{\nu n}\left\{\left(i_{\nu n} - \frac{i\omega c_n ii_{\nu n}}{U(1 - M^2)}\right)\bar{\gamma}_n + \left(j_{\nu n} - \frac{i\omega c_n jj_{\nu n}}{U(1 - M^2)}\right)\bar{\mu}_n\right\}, \qquad (62)$$

where $\nu = 0, \pm 1, \pm 2, \ldots \pm\frac{1}{2}(m - 1)$ represents the pivotal station $y = y_\nu = s\sin\{\nu\pi/(m + 1)\}$, and the odd integer m remains to be chosen. On substituting the two values $x = x_\nu'$, $x = x_\nu''$ from equation (56), the $2m$ complex linear equations will determine the $2m$ complex unknowns $\bar{\gamma}_n$, $\bar{\mu}_n$, $[n = 0, \pm 1, \pm 2, \ldots \pm\frac{1}{2}(m - 1)]$.

The real part of equation (62) is precisely the set of equations (27) in steady motion with incidence α replaced by a uniform value Q. These are expressed in the convenient form of equations (30), which yield an iterative solution for γ_n and μ_n. If the steady solution at unit incidence is denoted by $\bar{l} = l_1$, the solution of equations (62) may be written as

$$\bar{l} = Q\left(l_1 + \frac{i\omega\bar{c}}{U}l'\right), \qquad (63)$$

where terms of higher order in $\omega\bar{c}/U$ are ignored. To this order all the remaining terms in equation (62) are imaginary. On dividing throughout by the factor $i\omega\bar{c}Q/U$,

$$\frac{1}{b_{\nu\nu}}\left(\frac{x}{\bar{c}}\frac{1 - 2M^2}{1 - M^2} - \frac{x_0}{\bar{c}}\right) = (\bar{i}_{\nu\nu}\bar{\gamma}_\nu' + \bar{j}_{\nu\nu}\bar{\mu}_\nu') - \sum_{-\frac{1}{2}(m-1)}^{\frac{1}{2}(m-1)}{}' a_{\nu n}(i_{\nu n}\bar{\gamma}_n' + j_{\nu n}\bar{\mu}_n')$$

$$- \frac{1}{1 - M^2}\left[\left(\overline{ii}_{\nu\nu}\frac{(\bar{\gamma}_\nu)_1 c_\nu}{\bar{c}} + \overline{jj}_{\nu\nu}\frac{(\bar{\mu}_\nu)_1 c_\nu}{\bar{c}}\right)\right.$$

$$\left. - \sum_{-\frac{1}{2}(m-1)}^{\frac{1}{2}(m-1)}{}' a_{\nu n}\left(ii_{\nu n}\frac{(\bar{\gamma}_n)_1 c_n}{\bar{c}} + jj_{\nu n}\frac{(\bar{\mu}_n)_1 c_n}{\bar{c}}\right)\right],$$

where $(\bar{\gamma}_\nu)_1$, $(\bar{\mu}_\nu)_1$ correspond to steady conditions $\alpha = 1$. Then $\bar{\gamma}_n'$ and $\bar{\mu}_n'$, related to $\bar{l}'$ by an equation similar to (61), are identically the values corresponding to a steady incidence

$$\alpha' = \left(-\frac{x_0}{\bar{c}} + \frac{1 - 2M^2}{1 - M^2}\frac{x}{\bar{c}} + \frac{1}{1 - M^2}\alpha_3 \right), \quad \ldots \quad (64)$$

where

$$\alpha_3 = b_{\nu\nu}\left[\left(\overline{ii}_{\nu\nu}\frac{(\bar{\gamma}_\nu)_1 c}{\bar{c}} + \overline{jj}_{\nu\nu}\frac{(\bar{\mu}_\nu)_1 c_\nu}{\bar{c}}\right) - \sum_{-\frac{1}{2}(m-1)}^{\frac{1}{2}(m-1)}{}' a_{\nu n}\left(ii_{\nu n}\frac{(\bar{\gamma}_n)_1 c_n}{\bar{c}} + jj_{\nu n}\frac{(\bar{\mu}_n)_1 c_n}{\bar{c}}\right)\right].$$

Thus

$$\bar{l}' = \left(-\frac{x_0}{\bar{c}}\bar{l}_1 + \frac{1 - 2M^2}{1 - M^2}\bar{l}_2 + \frac{1}{1 - M^2}\bar{l}_3 \right), \quad \ldots \quad (65)$$

where

$\bar{l}_1$ corresponds to $\alpha_1 = 1$,
$\bar{l}_2$ corresponds to $\alpha_2 = x/\bar{c}$,
$\bar{l}_3$ corresponds to α_3 from equation (64).

Apart from the factor $(1 - 2M^2)/(1 - M^2)$, the first two terms in equation (65) are equivalent to a uniform rotation about the pitching axis $x = x_0$. The third term is a downwash due to the aerodynamic loading in phase with the pitching motion ; it represents a time lag between the loading and its induced downwash.

From equations (61), (63) and (65), the lift per unit area $\Delta p/\frac{1}{2}\rho U^2$ is the real part of

$$\left[\bar{l}_1\left(1 - \frac{i\omega x_0}{U}\right) + \bar{l}_2\frac{1 - 2M^2}{1 - M^2}\frac{i\omega\bar{c}}{U} + \bar{l}_3\frac{1}{1 - M^2}\frac{i\omega\bar{c}}{U}\right] Q \exp\left\{i\omega\left(t + \frac{xM^2}{U(1 - M^2)}\right)\right\}$$

$$= Q\exp(i\omega t)\left[\bar{l}_1 + \frac{i\omega\bar{c}}{U}\left(\frac{M^2}{1 - M^2}\frac{x}{\bar{c}}\bar{l}_1 - \frac{x_0}{\bar{c}}\bar{l}_1 + \frac{1 - 2M^2}{1 - M^2}\bar{l}_2 + \frac{1}{1 - M^2}\bar{l}_3\right)\right].$$

Then in phase with the pitching motion

$$\Delta p/\tfrac{1}{2}\rho U^2 = \mathscr{R}\{Q\bar{l}_1\exp(i\omega t)\},$$

i.e., from equation (58),

$$\Delta p/\tfrac{1}{2}\rho U^2 = \alpha\bar{l}_1. \quad \ldots \quad (66)$$

Out of phase with the pitching motion

$$\frac{\Delta p}{\frac{1}{2}\rho U^2} = \mathscr{R}\left\{\frac{i\omega Q\bar{c}}{U}\left(\frac{M^2}{1 - M^2}\frac{x}{\bar{c}}\bar{l}_1 - \frac{x_0}{\bar{c}}\bar{l}_1 + \frac{1 - 2M^2}{1 - M^2}\bar{l}_2 + \frac{1}{1 - M^2}\bar{l}_3\right)\exp(i\omega t)\right\},$$

i.e., from equation (58)

$$\frac{\Delta p}{\frac{1}{2}\rho U^2} = \frac{\dot{\theta}\bar{c}}{U}\left(\frac{M^2}{1 - M^2}\frac{x}{\bar{c}}\bar{l}_1 - \frac{x_0}{\bar{c}}\bar{l}_1 + \frac{1 - 2M^2}{1 - M^2}\bar{l}_2 + \frac{1}{1 - M^2}\bar{l}_3\right), \quad \ldots \quad (67)$$

where $\bar{l}_1$, $\bar{l}_2$, $\bar{l}_3$ are defined in equations (61) and (65).

The resulting derivatives of lift and pitching moment corresponding to equation (66) are given precisely by the formulae (31) and (34) in section 3. On substituting $\bar{\gamma}_1$, $\bar{\mu}_1$ for γ, μ in these formulae, let

$$\left.\begin{aligned} (C_L)_1 &= \frac{\pi A}{m + 1}\sum_{-\frac{1}{2}(m-1)}^{\frac{1}{2}(m-1)}(\bar{\gamma}_n)_1\cos\frac{n\pi}{m + 1} \\ (C_m)_1 &= \frac{\pi A^2}{2(m + 1)}\sum_{-\frac{1}{2}(m-1)}^{\frac{1}{2}(m-1)}\left\{(\bar{\mu}_n)_1\frac{c_n}{s} - (\bar{\gamma}_n)_1\left(\frac{x_{nl}}{s} + \frac{1}{4}\frac{c_n}{s}\right)\right\}\cos\frac{n\pi}{m + 1} \end{aligned}\right\}. \quad \ldots \quad (68)$$

However in calculating the coefficients corresponding to equation (67), the first term needs special treatment. Consider

$$\frac{\Delta p^*}{\frac{1}{2}\rho U^2} = \frac{x\bar{l}_1}{\bar{c}} = \frac{x}{\bar{c}}\left[\frac{8s\bar{\gamma}_1}{\pi c}\cot\tfrac{1}{2}\phi + \frac{32s\bar{\mu}_1}{\pi c}(\cot\tfrac{1}{2}\phi - 2\sin\phi)\right] \qquad \text{(69)}$$

and the corresponding coefficients

$$\left.\begin{aligned} C_L^* &= \int_{-s}^{s}\int_0^{\pi}\frac{x\bar{l}_1}{\bar{c}}\,\tfrac{1}{2}c\sin\phi\,d\phi\,\frac{dy}{2s\bar{c}} \\ C_m^* &= -\int_{-s}^{s}\int_0^{\pi}\frac{x\bar{l}_1}{\bar{c}}\,.\,x\,.\,\tfrac{1}{2}c\sin\phi\,d\phi\,\frac{dy}{2s\bar{c}^2}\,, \end{aligned}\right\} , \qquad \text{(70)}$$

where, measured from the apex,

$$x = x_l + \tfrac{1}{2}c(1 - \cos\phi).$$

Clearly

$$\begin{aligned} C_L^* &= \int_{-s}^{s}\int_0^{\pi}\bar{l}_1\,.\,x\,.\,\tfrac{1}{2}c\sin\phi\,d\phi\,\frac{dy}{2s\bar{c}^2} \\ &= -(C_m)_1 \text{ from equation (68)} \end{aligned} \qquad \text{(71)}$$

$$\begin{aligned} C_m^* &= -\frac{s}{\pi\bar{c}^3}\int_{-1}^{1}\int_0^{\pi}\{2\bar{\gamma}_1\cot\tfrac{1}{2}\phi + 8\bar{\mu}_1(\cot\tfrac{1}{2}\phi - 2\sin\phi)\}\times \\ &\qquad \{x_l + \tfrac{1}{2}c(1-\cos\phi)\}^2\sin\phi\,d\phi\,d\eta \\ &= -\frac{s}{\bar{c}^3}\int_{-1}^{1}[\bar{\gamma}_1(2x_l^2 + x_lc + \tfrac{1}{4}c^2) + \bar{\mu}_1(-4x_lc - \tfrac{3}{2}c^2)]\,d\eta \\ &= -\frac{A^2}{2}\int_{-1}^{1}\left[\bar{\gamma}_1\,.\,\frac{x_l^2 + \frac{1}{2}x_lc + \frac{1}{8}c^2}{\bar{c}s} - \bar{\mu}_1\frac{2x_lc + \frac{3}{4}c^2}{\bar{c}s}\right]d\eta \\ &= \frac{\pi A^2}{2(m+1)}\sum_{-\frac{1}{2}(m-1)}^{\frac{1}{2}(m-1)}\left[(\bar{\mu}_n)_1\frac{2x_{nl}c_n + \frac{3}{4}c_n^2}{\bar{c}s} - (\bar{\gamma}_n)_1\frac{x_{nl}^2 + \frac{1}{2}x_{nl}c_n + \frac{1}{8}c_n^2}{\bar{c}s}\right]\cos\frac{n\pi}{m+1}, \end{aligned} \qquad \text{(72)}$$

when the integration rule from Ref. 1, section 7, is applied. The last three terms of equation (67) are integrated to give formulae similar to (68). The aerodynamic coefficients may then be deduced from the pressure distributions.

The results are now expressed in terms of an 'equivalent wing' in incompressible flow. In the formulae (44) for the influence functions i and j, X is independent of M, but the spanwise parameter $Y = (1 - M^2)^{1/2}(y - y')/c(y')$. These influence functions are unchanged, if a wing with spanwise co-ordinates reduced by the factor $\sqrt{(1 - M^2)}$ is considered in incompressible flow. The pressure distribution is built up from terms $\bar{l}_1$, $\bar{l}_2$, $\bar{l}_3$, which are derived from solutions $(\bar{\gamma}_n)_1$, $(\bar{\mu}_n)_1$, etc., of the real part of equation (62), Q taking respective values α_1, α_2, α_3 from equation (65). α_1 and α_2 are independent of both M and spanwise co-ordinates ; and α_3 is invariant when the 'equivalent wing' is considered in incompressible flow. Hence $(\bar{\gamma}_n)_1$, $(\bar{\mu}_n)_1$, etc., are similarly invariant. The equivalent coefficients from equation (68) are obtained by substituting $s\sqrt{(1-M^2)}$ for s, and $A\sqrt{(1-M^2)}$ for A as follows:

$$\left.\begin{aligned} (I_L)_1 &= \frac{\pi A\sqrt{(1-M^2)}}{m+1}\sum_{-\frac{1}{2}(m-1)}^{\frac{1}{2}(m-1)}(\bar{\gamma}_n)_1\cos\frac{n\pi}{m+1} \\ (I_m)_1 &= \frac{\pi A^2\sqrt{(1-M^2)}}{2(m+1)}\sum_{-\frac{1}{2}(m-1)}^{\frac{1}{2}(m-1)}\left\{(\bar{\mu}_n)_1\frac{c_n}{s}-(\bar{\gamma}_n)_1\left(\frac{x_{nl}}{s}+\frac{1}{4}\frac{c_n}{s}\right)\right\}\cos\frac{n\pi}{m+1}\end{aligned}\right\}. \qquad (73)$$

Therefore from the term l_1,

$$\left.\begin{aligned}(C_L)_1 &= (I_L)_1/\sqrt{(1-M^2)} \\ (C_m)_1 &= (I_M)_1/\sqrt{(1-M^2)}\end{aligned}\right\}. \qquad (74)$$

Similar equations hold for l_2 and l_3; and from equation (72),

$$C_m{}^* = I_m{}^*/\sqrt{(1-M^2)} = \frac{1}{\sqrt{(1-M^2)}}\frac{\pi A^2(1-M^2)}{2(m+1)}\sum_{-\frac{1}{2}(m-1)}^{\frac{1}{2}(m-1)}\left[(\bar{\mu}_n)_1\frac{2x_{nl}c_n+\frac{3}{4}c_n{}^2}{\bar{c}s\sqrt{(1-M^2)}}\right.$$

$$\left.-(\bar{\gamma}_n)_1\frac{x_{nl}{}^2+\frac{1}{2}x_{nl}c_n+\frac{1}{8}c_n{}^2}{\bar{c}s\sqrt{(1-M^2)}}\right]\cos\frac{n\pi}{m+1}, \qquad (75)$$

where s and A refer to the actual wing.

From equations (68) and (72), the pressure distribution out of phase with the pitching motion in equation (67) gives a lift coefficient

$$C_L = \frac{\dot{\theta}\bar{c}}{U}\left(-\frac{M^2}{1-M^2}C_L{}^* - \frac{x_0}{\bar{c}}(C_L)_1 + \frac{1-2M^2}{1-M^2}(C_L)_2 + \frac{1}{1-M^2}(C_L)_3\right)$$

$$= \frac{\dot{\theta}\bar{c}}{U}\left(\frac{M^2}{(1-M^2)^{3/2}}(I_m)_1 - \frac{1}{(1-M^2)^{1/2}}\frac{x_0}{\bar{c}}(I_L)_1 + \frac{1-2M^2}{(1-M^2)^{3/2}}(I_L)_2\right.$$

$$\left.+\frac{1}{(1-M^2)^{3/2}}(I_L)_3\right) \qquad (76)$$

in terms of the 'equivalent wing.' Similarly the moment coefficient about the pitching axis $x = x_0$ is

$$(C_m)_0 = C_m + \frac{x_0}{\bar{c}}C_L,$$

where referred to the axis $x = 0$ through the leading edge of the central section

$$C_m = \frac{\dot{\theta}\bar{c}}{U}\left\{\frac{M^2}{(1-M^2)^{3/2}}I_m{}^* - \frac{1}{(1-M^2)^{1/2}}\frac{x_0}{\bar{c}}(I_m)_1 + \frac{1-2M^2}{(1-M^2)^{3/2}}(I_m)_2\right.$$

$$\left.+\frac{1}{(1-M^2)^{3/2}}(I_m)_3\right\}. \qquad (77)$$

Then the pitching derivatives are defined by

$$z_\theta = -\frac{1}{2}\frac{\partial C_L}{\partial(\theta\bar{c}/U)} = -\frac{1}{2}\left[\left(-\frac{1-\beta^2}{\beta^3}(I_m)_1 + \frac{2\beta^2-1}{\beta^3}(I_L)_2 + \frac{1}{\beta^3}(I_L)_3\right) - \frac{x_0}{\bar{c}}\frac{1}{\beta}(I_L)_1\right] \quad \ldots \quad (78)$$

$$m_\theta = \frac{1}{2}\frac{\partial (C_m)_0}{\partial(\theta\bar{c}/U)} = \frac{1}{2}\left[\left(\frac{1-\beta^2}{\beta^3}I_m{}^* + \frac{2\beta^2-1}{\beta^3}(I)_{m2} + \frac{1}{\beta^3}(I_m)_3\right) + \frac{x_0}{\bar{c}}\left(-\frac{1}{\beta^3}(I_m)_1 + \frac{2\beta^2-1}{\beta^3}(I_L)_2 + \frac{1}{\beta^3}(I_L)_3\right) - \left(\frac{x_0}{\bar{c}}\right)^2\frac{1}{\beta}(I_L)_1\right], \quad \ldots \quad (79)$$

where $\beta = \sqrt{(1 - M^2)}$ and in accordance with equation (74) I_L and I_m are coefficients of lift and pitching moment for the 'equivalent wing' in incompressible flow. Thus, when $M = 0$, the pitching derivatives become

$$\left.\begin{aligned} z_\theta &= -\frac{1}{2}\left[\{(C_L)_2 + (C_L)_3\} - \frac{x_0}{\bar{c}}(C_L)_1\right] \\ m_\theta &= \frac{1}{2}\left[\{(C_m)_2 + (C_m)_3\} + \frac{x_0}{\bar{c}}\{-(C_m)_1 + (C_L)_2 + (C_L)_3\} - \left(\frac{x_0}{\bar{c}}\right)^2 (C_L)_1\right] \end{aligned}\right\} \quad \ldots \quad (80)$$

The stages of evaluating z_θ and m_θ may be summarized as follows :

(i) Given the plan-form and the Mach number, determine the 'equivalent wing' of semi-span $s\sqrt{(1 - M^2)}$.

(ii) Calculate $\bar{l}_1$ and $\bar{l}_2$ corresponding to incidences $\alpha_1 = 1$ and $\alpha_2 = x/\bar{c}$ by the method of Ref. 1 (modified slightly to make use of the new tables of i and j in Ref. 11).

(iii) Calculate α_3 from equation (64) by using the additional influence functions ii and jj and the values of $\bar{y}$ and $\bar{\mu}$ corresponding to $\bar{l}_1$.

(iv) Calculate $\bar{l}_3$ corresponding to α_3 as in stage (ii).

(v) Evaluate the coefficients of lift and pitching moment corresponding to $\bar{l}_1$, $\bar{l}_2$, $\bar{l}_3$ from equations (68) and the special term $I_m{}^*$ from equation (75). Note: The symbol I replaces the usual C as a reminder of stage (i).)

(vi) Evaluate the derivatives z_θ and m_θ from equations (78) and (79).

For further computational details the reader is referred to Appendix VII of Ref. 1 and Appendix I of this report.

6. *Numerical Results.*—For the reasons given in section 1 the present calculations include five plan-forms : one circular ; one arrowhead ($A = 1\cdot32$), Wing 9 ; and three delta ($A = 1\cdot2$, 2, 3), Wings 0, 1, 2 respectively. The numbers correspond to Ref. 6, Fig. 1. The three related delta wings of taper ratio $\lambda = 1/7$ have been chosen to illustrate the effects of aspect ratio and compressibility. Wings 1 and 0 are 'equivalent' to Wing 2 at $M = 0\cdot745$ and $M = 0\cdot917$ respectively in the sense indicated above equation (73).

Before proceeding with any calculations it is necessary to specify m, the number of spanwise variablés. With a single exception (Wing 2 with $m = 7$) the recommendation of Ref. 1, $m > 3A$, has been followed. The circular plate and Wings 9 and 2 have each been calculated for two different values of m.

Throughout, the influence functions i and j have been determined from enlarged charts similar to Figs. 1 to 6 of Ref. 1, which were based on some calculations by M. Winter. He also provided unpublished tables of ii and jj for certain values of Y, which have been used to evaluate α_3 from equation (64). As explained at the end of section 3, a complete tabulation of i, j, ii, jj has been carried out by the staff of the Mathematics Division of the N.P.L. (Ref. 11). A check calculation in the particular case of Wing 2 with $m = 7$ has shown that Ref. 11 gives much more reliable values of the influence functions. However the recalculated derivatives z_θ and m_θ differ from the values given in Table 4 by at most $0 \cdot 002$ over the whole range of pitching axis $0 < x_0 < 1 \cdot 75\bar{c}$. It has therefore been assumed that the computational accuracy is of this order in the other seven cases considered.

The present calculations are summarized in Table 1. Each of the eight solutions for the derivatives is fully expressed by the seven coefficients

$$(I_L)_1, \quad (I_L)_2, \quad (I_L)_3, \quad I_L{}^* = -(I_m)_1, \quad -(I_m)_2, \quad -(I_m)_3, \quad -I_m{}^*,$$

the last of which only occurs in compressible flow. The derivatives z_θ and m_θ may then be determined from equations (78) and (79). Their values have been tabulated against the position of pitching axis in Tables 2, 3, 4, 5 and 6. It will be seen that the derivatives in Table 2 for the circular plate are specially defined in terms of the radius R.

There are three distinct considerations arising from these results :

(i) the number of spanwise terms, m ;

(ii) the effect of aspect ratio ($M = 0$) ;

(iii) the effect of compressibility.

The numerical implications of each will be discussed.

6.1. *The Number of Spanwise Terms.*—The choice of m affects the accuracy with which the spanwise integrations are achieved. From section 3 the technique used by Multhopp in the 'lifting-line' theory results in the formula (24), but a lifting surface introduces one or two complications :

(*a*) a logarithmic singularity in the second derivative of the integrand ;

(*b*) a divergent integral when the leading or trailing edge is kinked.

(*a*) is always present ; and the correction, included in equation (27), is probably satisfactory so long as the wing is not highly tapered, when the refinement of Ref. 13 is important, (*b*) is absent for the circular plate ; but each of the other examples involves an 'interpolated wing' with a change in plan-form near the central section from equation (28). Both of these complications are treated by devices dependent on the choice of m.

It might be expected that m would matter less for the circular plate than for the delta wing with a kinked leading edge, and would become more significant for the arrowhead wing whose trailing edge is kinked as well. Such effects are apparent from the coefficients in Table 1. The largest discrepancy of all, occurring for the arrowhead wing, is the change in $-(I_m)_3$ from $0 \cdot 70$ to $0 \cdot 81$ as m is reduced from 11 to 5.

However, when the pitching derivatives in incompressible flow are compared in Tables 2, 3 and 4, the differences are rather smaller than Table 1 would suggest. In Fig. 1 the unbroken curves for the circular plate for the two values $m = 7$ and $m = 5$ are in excellent agreement. The largest effect of m is recorded in Fig. 2 for the arrowhead wing with pitching axis through the leading apex, when increases of $0 \cdot 10$ (6 per cent) in $-z_\theta$ and $0 \cdot 07$ (4 per cent) in $-m_\theta$

occur as m is reduced from 11 to 5. Fig. 3 shows that the least favourable pitching axis for the delta wing is $x_0 = 1 \cdot 3\bar{c}$; a decrease in m from 15 to 7 then changes $- z_\theta$ by $+ 0 \cdot 04$ (6 per cent) and $- m_\theta$ by $- 0 \cdot 03$, a reduction of about 20 per cent in the minimum damping.

These differences are considerably smaller than those between the present theory and other oscillatory theories (section 8) and amount to less than a quarter of the corrections to the steady theory (section 7). The effects of m leave scope for improvement, but the numerical inconsistencies on that account are encouragingly small and of little importance to a practical aerodynamicist.

6.2. *The Effect of Aspect Ratio*.—To some extent aspect ratio determines the labour of computation. For an isolated problem it would be unwise to choose a value of m less than $3A$; and for a swept wing m should be at least 7. A reasonable estimate of computational time on a desk calculator is $0 \cdot 08m^2$ days ; this covers all stages of the work (Appendix II) including the initial steady theory of Ref. 1. Thus for any particular swept wing the calculations might be expected to take at least $0 \cdot 7A^2$ days and not less than 4 days. The method is best suited to wings of moderately small aspect ratio, for which it is relatively quick compared with the 7 weeks of computation, when $A > 5$ and it is advisable to take $m = 23$.

From the few calculations of the derivatives themselves no general conclusions about the effect of aspect ratio can be drawn. However, in the particular case of delta wings with a taper ratio of 1/7, Fig. 4 shows that A has a marked effect on z_θ. For the practical range of pitching axis $0 \cdot 75\bar{c} < x_0 < 1 \cdot 10\bar{c}$ there is a reduction of the order $0 \cdot 26$ (22 per cent) in $- z_\theta$ as A changes from 3 to $1 \cdot 2$. The corresponding reduction of $0 \cdot 05$ (14 per cent) in $- m_\theta$, though barely significant, is confirmed by experiment (section 9).

The low aspect ratio theory given by Garrick[12] (1951) is considered in Appendix III, where formulae

$$\left.\begin{aligned} z_\theta &= -\pi A \left(\frac{5}{8} - \frac{1}{4}\frac{x_0}{\bar{c}}\right) \\ m_\theta &= -\pi A \left\{\frac{7}{8} - \frac{1}{2}\left(\frac{x_0}{\bar{c}}\right)\right\}^2 \end{aligned}\right\} \qquad \ldots \quad (81)$$

are derived for the family of delta wings ($\lambda = 1/7$). It is quite clear from Table 5 and Fig. 4 that even for A as low as $1 \cdot 2$ neither z_θ nor m_θ is approximately proportional to A. The formulae (81) differ from the numerical results of Multhopp's theory by as much as $0 \cdot 43$ (100 per cent) even for $A = 1 \cdot 2$, and the discrepancies become more serious with increasing A. When $A < 0 \cdot 5$, the formulae are apparently more consistent ; and the dotted curves for $A = 0 \cdot 5$, shown in Fig. 4, match the other three curves fairly well. Better indications of the validity of the formulae (81) for z_θ and m_θ are given respectively in Figs. 6 and 7, where the derivatives are plotted against A for three pitching axes $x_0 = 0 \cdot 5\bar{c}$, $0 \cdot 973\bar{c}$, $1 \cdot 4\bar{c}$. The dotted curves from (81) roughly approximate to the numerical results for incompressible flow ($M = 0$) at very low aspect ratios. But they are seldom likely to supplant the more exact calculations.

6.3. *The Effect of Compressibility*.—The present theory is valid provided that $\omega\bar{c}M/U(1 - M^2)$ is small compared with unity ; the method is thus inapplicable to practical values of ω at very high subsonic speeds. A change of Mach number involves a change in the 'equivalent wing' of aspect ratio $A\sqrt{(1 - M^2)}$. Computations at higher M will therefore tend to be shorter (section 6.2).

The calculations for the family of delta wings determine the pitching derivatives for Wing 2 ($A = 3$) at $M = 0$, $0 \cdot 745$, $0 \cdot 917$ (Table 6). The unbroken curves of z_θ against $x_0/\bar{c}$ in Fig. 5 are separated by much the same amount as the curves of z_θ in Fig. 4. But whereas A has little effect in the region $1\cdot2\bar{c} < x_0 < 1\cdot4\bar{c}$, the effect of M almost disappears when $0\cdot2\bar{c} < x_0 < 0\cdot6\bar{c}$. Fig. 8 shows typical theoretical curves of z_θ against M. There is evidence from Fig. 6 that for wings of low aspect ratio z_θ is not sensitive to M, whatever the pitching axis.

On the other hand the results plotted in Fig. 5 show that the effect of M on m_θ is much greater than the equivalent effect of A in Fig. 4. For the practical range of pitching axis $0\cdot75\bar{c} < x_0 < 1\cdot10\bar{c}$ there is an increase of the order $0\cdot58$ (160 per cent) in $-m_\theta$ as M changes from 0 to $0\cdot917$, while the corresponding increase in $-m_\theta$ from experiment is about $0\cdot45$ (Fig. 8). Thus the effect of compressibility up to $M = 0\cdot9$ is fairly well predicted by theory despite the presence of shock-waves. Theoretical curves of m_θ against A for $M = 0$, $0\cdot6$, $0\cdot8$, $0\cdot9$, $0\cdot95$ are shown in Fig. 7. The general appearance is surprisingly sensitive to pitching axis. The usual effect of M is towards greater stability; the interesting exception, however, is the case of high M and high A with a forward pitching axis, when compressibility can produce a theoretical tendency towards negative damping.

7. *Comparisons with Steady Derivatives.*—The oscillatory derivatives z_θ and m_θ are given in equations (78) and (79). These formulae will be compared with those corresponding to a uniform pitching rotation.

7.1. *Steady Pitching Derivatives.*—For a steady rate of pitching q the boundary condition in place of equation (59) is

$$w = -q(x - x_0)\,. \qquad (82)$$

This is equivalent to an incidence

$$\alpha(x) = -\frac{w}{U} = -\frac{qx_0}{U}\alpha_1 + \frac{q\bar{c}}{U}\alpha_2\,,$$

where

$$\left.\begin{aligned} \alpha_1 &= 1 \\ \alpha_2 &= x/c \end{aligned}\right\}.$$

Then, in the notation of equation (65), the non-dimensional load is

$$l = \frac{\Delta p}{\frac{1}{2}\rho U^2} = -\frac{qx_0}{U}l_1 + \frac{q\bar{c}}{U}l_2\,. \qquad (83)$$

Then from equations (73) and similar ones for $(I_L)_2$ and $(I_m)_2$ corresponding to l_2

$$C_L = \frac{q\bar{c}}{U}\left(-\frac{1}{\sqrt{(1-M^2)}}\frac{x_0}{\bar{c}}(I_L)_1 + \frac{1}{\sqrt{(1-M^2)}}(I_L)_2\right), \qquad (84)$$

$$(C_m)_0 = \frac{x_0}{\bar{c}}C_L + \frac{q\bar{c}}{U\sqrt{(1-M^2)}}\left(-\frac{x_0}{\bar{c}}(I_m)_1 + (I_m)_2\right). \qquad (85)$$

Thus by treating equation (83) similarly to (67) the steady derivatives are obtained at once

$$z_q = -\frac{1}{2}\frac{\partial C_L}{\partial(q\bar{c}/U)} = -\frac{1}{2\beta}\left((I_L)_2 - \frac{x_0}{\bar{c}}(I_L)_1\right), \qquad (86)$$

$$m_q = \frac{1}{2}\frac{\partial (C_m)_0}{\partial(q\bar{c}/U)} = \frac{1}{2\beta}\left[(I_m)_2 + \frac{x_0}{\bar{c}}\{-(I_m)_1 + (I_L)_2\} - \left(\frac{x_0}{\bar{c}}\right)^2(I_L)_1\right], \qquad (87)$$

where $\beta = \sqrt{(1 - M^2)}$ and the coefficients I_L and I_m correspond to the 'equivalent wing' in incompressible flow. When $M = 0$, the derivatives of lift and pitching moment on a steadily pitching wing become

$$\left.\begin{aligned} z_q &= -\frac{1}{2}\left((C_L)_2 - \frac{x_0}{\bar{c}}(C_L)_1\right) \\ m_q &= \frac{1}{2}\left[(C_m)_2 + \frac{x_0}{\bar{c}}\{-(C_m)_1 + (C_L)_2\} - \left(\frac{x_0}{\bar{c}}\right)^2 (C_L)_1\right] \end{aligned}\right\} , \quad \ldots \quad \ldots \quad (88)$$

which should be compared with the oscillatory derivatives in incompressible flow as given by equations (80). These only differ from (88) in that extra terms $(C_L)_3$ and $(C_m)_3$ include the time lag in downwash due to the aerodynamic loading in phase with the pitching motion. However in compressible flow there is a further effect on account of the retarded frequency, which gives rise to the first term in equation (67) and the coefficients $C_L{}^*$ and $C_m{}^*$.

7.2. *Numerical Comparisons.*—The summary of the present calculations in Table 1 includes the four coefficients

$$(I_L)_1,\ (I_L)_2,\ -(I_m)_1,\ -(I_m)_2,$$

which determine the steady derivatives defined in equations (86) and (87). The last columns of Tables 2, 3 and 4 give values of z_q and m_q in incompressible flow ($\beta = 1$) for the circular plate, arrowhead wing ($A = 1\cdot32$) and delta wing ($A = 3$) respectively. In each case the larger value of m has been taken. The tabulated values of z_q and m_q may be compared with the derivatives z_θ and m_θ from equation (80) for the range of pitching axis.

The plotted comparisons in Figs. 1, 2 and 3 show that the difference between the steady and oscillatory derivatives varies a lot with plan-form. For the circular plate the displacement in the lift derivative is given by

$$-\frac{R}{\bar{c}}(z_\theta - z_q) = \tfrac{1}{2}(I_L)_3 = 0\cdot49\ ,$$

which is considerably larger than the corresponding values of $0\cdot30$ for the arrowhead wing and $0\cdot25$ for the delta wing. This partly explains why the pitching-moment derivatives for the circular plate in Fig. 1 differ so much. Nevertheless m_θ and m_q happen to be in close agreement for the diametric pitching axis $x_0 = R$.

Equations (80) and (88) show that the minimum $-m_\theta$ occurs when the pitching axis is at a distance

$$(\Delta x_0) = \tfrac{1}{2}\bar{c}(I_L)_3/(I_L)_1 \quad \ldots \quad \ldots \quad \ldots \quad \ldots \quad \ldots \quad \ldots \quad \ldots \quad \ldots \quad (89)$$

behind the position for minimum $-m_q$. The value of the minimum is reduced in magnitude by an amount

$$\begin{aligned} (\Delta m) &= (-m_q)_{\text{min.}} - (-m_\theta)_{\text{min.}} \\ &= \tfrac{1}{2}(I_m)_3 + \tfrac{1}{4}(I_L)_3\{-(I_m)_1 + (I_L)_2 + \tfrac{1}{2}(I_L)_3\}/(I_L)_1\,. \quad \ldots \quad \ldots \quad \ldots \quad (90) \end{aligned}$$

Then, starting from a curve of $-m_q$ against $x_0/\bar{c}$, the oscillatory derivative $-m_\theta$ is obtained by translating the curve $(\Delta x_0)/\bar{c}$ to the right (x_0 increasing) and (Δm) upwards ($-m_\theta$ decreasing). The derivatives for the circular plate are defined in terms of R in Table 2. Thus (Δm) is multiplied by the special factor

$$(\bar{c}/R)^2 = \pi^2/4,$$

which would appear on the right-hand side of equation (90).

Wing	m	A	$(\Delta x_0)/\bar{c}$	(Δm)
Circle	7	1·27	0·267	0·053
Circle	5	1·27	0·272	0·059
Arrowhead	11	1·32	0·186	0·061
Arrowhead	5	1·32	0·210	0·072
Delta	15	3·00	0·081	−0·001
Delta	7	3·00	0·098	0·037
Delta	7	2·00	0·172	0·077
Delta	7	1·20	0·235	0·090

It seems that both $(\Delta x_0)/\bar{c}$ and (Δm) increase when the aspect ratio is reduced. Although the steady and oscillatory curves for the delta wing ($A = 3$) in Fig. 3 are not far separated, the comparison for the arrowhead wing in Fig. 2 is probably more typical of swept wings of moderately low aspect ratio. Quite generally in incompressible flow the curves of m_θ and m_q cross where $x_0/\bar{c} = -(I_m)_3/(I_L)_3$, which is found at roughly $0 \cdot 2\bar{c}$ behind the aerodynamic centre. Therefore in practice the damping of pitching oscillations can be expected to be greater than the derivative m_q would suggest.

A more direct indication of the difference between oscillatory and purely rotational flow is the magnitude of the incidence α_3, which constitutes the phase lag between the wing loading and the induced downwash. A summary of values is contained in Table 7, where it is shown that α_3 can take large values, positive at the central section ($\eta = 0$) and negative near the tip ($\eta = 1$). From equation (65) the magnitudes of the tabulated α_3 and $\alpha_2 = x/\bar{c}$ are of equal importance in determining the loading out of phase with the pitching motion. At $\eta = 0$ in particular the ratio of α_3' (at $0 \cdot 9045c$) to α_2' is as much as 0·75. It is the change in sign of α_3 over the outer span that accounts for the smaller ratios of $(I_L)_3/(I_L)_2$ and $(I_m)_3/(I_m)_2$ from Table 1. Consequently the effect on the out-of-phase wing loading in incompressible flow is more significant than the comparative derivatives indicate.

Steady pitching ceases to be a useful guide when the effects of compressibility are important and the additional coefficients $C_L{}^*$ and $C_m{}^*$ come into play. These coefficients, however, are given in equations (71) and (72) in terms of the steady solution for unit incidence. Results for the delta wing ($A = 3$) in Fig. 5 show that the curves of z_θ and z_q for a given Mach number remain parallel, but that the difference $z_\theta - z_q$ changes sign at approximately $M = 0 \cdot 78$. Thus the z_θ curves converge for a forward pitching axis, while the z_q curves converge for a pitching axis near the trailing edge.

The curve of the oscillatory derivative m_θ for $M = 0 \cdot 917$, $x_0/\bar{c} > 0 \cdot 7$ in Fig. 5 illustrates how much the effect of compressibility can be underestimated by the steady theory. For the practical range of pitching axis, $0 \cdot 75\bar{c} < x_0 < 1 \cdot 10\bar{c}$, as M changes from 0 to 0·917, the average increase in $-m_\theta$ of 0·58 compares with the much smaller value of 0·23 for the steady $-m_\theta$. Experiments on the delta wing (Fig. 8) give a corresponding increase in $-m_\theta$ of about 0·45 and support the larger value from the oscillatory theory of limiting frequency.

8. *Comparisons with Other Theories.*—Three oscillatory theories are considered in the light of the present calculations :

Ref. 5 (Miss Lehrian) ;

Ref. 7 (Schade and Krienes) ;

Ref. 8 (Kochin).

The last two of these are particular solutions for the oscillating circular plate. Ref. 5 is of general application ; and results for the circular plate, arrowhead wing and delta wing ($A = 3$) are quoted in Tables 2, 3 and 4 respectively.

8.1. *Circular Aerofoil.*—The circular aerofoil was chosen as one of the present examples because the independent solutions of Schade and Krienes[7] and Kochin[8] were available.

From page 29 of Ref. 7 the expressions for the lift and pitching moment in the present notation (section 12) become

$$\left.\begin{aligned} L &= \mathscr{R}\left\{\pi\rho U^2R^2\frac{8}{\pi}\left(\frac{2}{3}i\Omega + K_{s0} + \frac{2}{3}i\Omega K_{k0}\right)Q\exp(i\omega t)\right\} \\ \mathscr{M}_0 &= \mathscr{R}\left\{-\pi\rho U^2R^2\frac{8}{3\pi}\left(-\frac{2}{15}\Omega^2 + K_{s1} + \frac{2}{3}i\Omega\, K_{k1}\right)Q\exp(i\omega t)\right\} \end{aligned}\right\}, \qquad (91)$$

where Ω denotes $\omega R/U$ and the instantaneous incidence about the axis $x_0 = R$ satisfies

$$\left.\begin{aligned} \alpha &= \mathscr{R}\{Q\exp(i\omega t)\} \\ \partial\alpha/\partial t = \dot{\theta} &= \mathscr{R}\{i\omega Q\exp(i\omega t)\} \end{aligned}\right\}.$$

From Tables 1 and 2 of Ref. 7, in the limit as $\omega \rightarrow 0$,

$$\left.\begin{aligned} K_{s0} &= 0\cdot3531 - 0\cdot2484\, i\Omega \\ K_{s1} &= -0\cdot5489 + 0\cdot4465\, i\Omega \\ K_{k0} &= -0\cdot2221 + 0\cdot1259\, i\Omega \\ K_{k1} &= 0\cdot3872 - 0\cdot2630\, i\Omega \end{aligned}\right\} \quad \ldots \quad (92)$$

Therefore, on proceeding to the limit, equations (91) and (92) give

$$\left.\begin{aligned} C_L &= \frac{16}{\pi}\left(0\cdot3531\alpha + 0\cdot2702R\dot{\theta}/U\right) = 1\cdot798\alpha + 0\cdot688(2R\dot{\theta}/U) \\ (C_m)_0 &= -\frac{16}{3\pi}\frac{R}{\bar{c}}\left(-0\cdot5489\alpha + 0\cdot7046R\dot{\theta}/U\right) = 0\cdot593\alpha - 0\cdot598(2R^2\dot{\theta}/U\bar{c}) \end{aligned}\right\}, \qquad (93)$$

when the pitching axis is $x_0 = R$. The corresponding values of $\partial C_L/\partial\alpha = 1\cdot788$ and $\partial(C_m)_0/\partial\alpha = 0\cdot597$ by Multhopp's steady lifting-surface theory are in excellent agreement. However the derivatives $-z_\theta = 1\cdot219$ and $-m_\theta = 0\cdot244$ in Table 2 are very different from the respective values $0\cdot688$ and $0\cdot598$ given in equation (93). About a general pitching axis Schade and Krienes give

$$\left.\begin{aligned} -z_\theta &= 1\cdot587 - 0\cdot899x_0/R \\ -m_\theta &= 1\cdot720 - 2\cdot021x_0/R + 0\cdot899(x_0/R)^2 \end{aligned}\right\} \quad \ldots \quad (94)$$

The results of Kochin's theory are given in equations (4.1), (4.42) and (4.43) of Ref. 8, Part I. In the present notation, the lift and pitching moment on a flat circular wing in periodic oscillations of small frequency about a diametric pitching axis are respectively

$$\left.\begin{aligned} L &= \rho U^2R^2(2\cdot813\alpha + 1\cdot766R\dot\theta/U) \\ \mathscr{M}_0 &= \rho U^2R^3(1\cdot473\alpha - 0\cdot867R\dot\theta/U) \end{aligned}\right\}.$$

Hence

$$\left.\begin{aligned} C_L &= 1\cdot791\alpha + 0\cdot562(2R\dot\theta/U) \\ (C_m)_0 &= 0\cdot597\alpha - 0\cdot276(2R^2\dot\theta/U\bar{c}) \end{aligned}\right\}, \qquad (95)$$

when the pitching axis is $x_0 = R$. Again $\partial C_L/\partial\alpha$ and $\partial(C_m)_0/\partial\alpha$ are in excellent agreement with the values from Multhopp's lifting-surface theory. In the special notation of Table 2, Kochin's values of the oscillatory derivatives for a general pitching axis are given by

$$\left.\begin{aligned} -\, z_{\dot\theta} &= 1\cdot457 - 0\cdot895x_0/R \\ -\, m_{\dot\theta} &= 1\cdot265 - 1\cdot884x_0/R + 0\cdot895(x_0/R)^2 \end{aligned}\right\}. \qquad (96)$$

From equations (94) and (96) the curves of $z_{\dot\theta}$ and $m_{\dot\theta}$ against x_0/R in Fig. 1 show that neither Ref. 7 nor Ref. 8 supports the present theory ; in fact the results of Ref. 8 lie fairly close to the steady pitching derivatives from section 7.1.

The calculations from Ref. 5, however, agree favourably with Multhopp's oscillatory theory. Close comparisons for both derivatives are shown in Table 2 and Fig. 1. These cast doubt on the results given in Refs. 7 and 8 and point to the desirability of checking the complicated analysis in both of these methods.

8.2. *Vortex-Lattice Technique.*—The first routine for an oscillatory lifting-surface theory was suggested by W. P. Jones[2] (1946). His method yields a practicable computation for high frequencies by developing the vortex-lattice technique[3] (Falkner, 1943) to evaluate periodic downwashes. Miss Lehrian has modified the theory of Ref. 2 to permit the calculation of stability derivatives of low frequency in Ref. 5, whence values for three wings in incompressible flow are placed alongside the present results in Tables 2, 3 and 4. As mentioned above (section 8.1), the comparisons in Table 2 for the oscillating circular plate are good.

Whereas the computation in Multhopp's theory is specific once m is fixed, the method of Ref. 5 involves an arbitrary lattice and choice of both the number and combination of pivotal points. In the more crucial case of swept wings this choice demands experience, since it may be expected to affect the numerical results. Those quoted for the arrowhead wing in Table 3 and the delta wing in Table 4 correspond to a 21 × 6 lattice with a total of 6 pivotal points situated at $\frac{1}{2}c$ and $\frac{5}{6}c$.

For forward pitching axes the two theories agree well, but for axes closely behind the calculated aerodynamic centre differences begin to become appreciable. For $x_0 = \bar{c}$ in Fig. 3, Ref. 5 gives a value of $-m_{\dot\theta}$ for the delta wing $0\cdot05$ (17 per cent) greater than the present theory. Such discrepancies continue to grow with increasing x_0 until the estimated damping about a pitching axis near the trailing edge differs by as much as $0\cdot18$ (40 per cent). This trend appears in Figs. 1, 2 and 3, and in each case involves discrepancies between the two theories of at least three times the calculated effect of varying m in the present theory.

From the general standpoint the comparisons between the present theory and vortex-lattice technique are encouraging. It seems that the margin of uncertainty in stability derivatives has been greatly narrowed down. In conjunction the two theories provide a foundation on which the effects of high frequency can be superposed through Ref. 4 and further applications of Ref. 2.

9. *Comparisons with Experiment.*—Measured values of $m_{\dot{\theta}}$ for the delta wing ($A = 3$) have been found by two totally different experimental techniques. Results at low speed obtained at R.A.E. for two complete models[14] (Moss, 1952) compare well with those obtained at N.P.L. for a half-model tested over the range of speed $0 \cdot 40 < M < 0 \cdot 90$. The results plotted against M in Fig. 8 correspond to oscillations about the two pitching axes, $x_0 = 0 \cdot 973\bar{c}$ and $x_0 = 0 \cdot 754\bar{c}$, with zero mean incidence. At all speeds the derivative was approximately independent of frequency provided that the parameter $\omega\bar{c}/U > 0 \cdot 03$. The measurements at R.A.E. were made on different sized models, both of which described pitching oscillations about the axes $x_0 = 0 \cdot 664\bar{c}$ and $x_0 = 0 \cdot 937\bar{c}$. The results are taken from Fig. 18 of Ref. 14, where there was no indication of any marked change in $m_{\dot{\theta}}$ throughout the range $0 \cdot 03 < \omega\bar{c}/U < 0 \cdot 16$, which includes the highest experimental frequency. The following average values of the derivative are plotted against $x_0/\bar{c}$ in Fig. 3, where they confirm the theoretical values ($m = 15$) for the delta wing ($A = 3$) in incompressible flow :

Model	Span $2s$ (ft)	Pitching axis x_0	Values of $-m_{\dot{\theta}}$	
			Measured	Theoretical
Complete	5·485	$0 \cdot 664\bar{c}$	0·69	0·756
Complete	5·485	$0 \cdot 937\bar{c}$	0·32	0·340
Complete	3·35	$0 \cdot 664\bar{c}$	0·73	0·756
Complete	3·35	$0 \cdot 937\bar{c}$	0·37	0·340
Half ($M = 0 \cdot 4$)	0·571	$0 \cdot 754\bar{c}$	0·52	0·594
Half ($M = 0 \cdot 4$)	0·571	$0 \cdot 973\bar{c}$	0·30	0·302

Fig. 3 includes a dotted experimental curve of $m_{\dot{\theta}}$ from Fig. 26 of Ref. 14, which is used to obtain values at $M = 0$ in Fig. 8.

Measurements on oscillating models of the arrowhead wing ($A = 1 \cdot 32$) and the delta wing ($A = 1 \cdot 2$) have been made at low speed in the N.P.L. Low-turbulence Tunnel[15, 16] (Scruton, Woodgate and Alexander, 1953). For both wings the lift derivative $-z_{\dot{\theta}}$ and the damping $-m_{\dot{\theta}}$ have been measured for two pitching axes. Oscillations with zero mean incidence showed no effect of amplitude on these derivatives ; and marked effects of frequency were confined to low values of the parameter $\omega\bar{c}/U$. Within experimental scatter the derivatives were constant throughout the ranges of frequency

$0 \cdot 25 < \omega\bar{c}/U < 0 \cdot 75$ for the arrowhead wing (Ref. 16),

$0 \cdot 15 < \omega\bar{c}/U < 0 \cdot 50$ for the delta wing (Ref. 15).

Thus with zero mean incidence the experimental $-z_{\dot{\theta}}$ and $-m_{\dot{\theta}}$ were virtually independent of both frequency and amplitude at the higher frequencies $\omega\bar{c}/U > 0 \cdot 20$ for the range of amplitude $1 \cdot 5$ deg $< Q < 4 \cdot 5$ deg and the average values are given in the following table :

Wing	A	Pitching axis x_0	$-z_{\dot{\theta}}$	$-m_{\dot{\theta}}$
Arrowhead	1·32	$0 \cdot 883\bar{c}$	0·75	0·27
Arrowhead	1·32	$1 \cdot 063\bar{c}$	0·55	$0 \cdot 13_5$
Delta	1·2	$0 \cdot 754\bar{c}$	1·01	0·49
Delta	1·2	$0 \cdot 973\bar{c}$	$0 \cdot 85_5$	$0 \cdot 26_5$

These derivatives have not been corrected for tunnel interference, which is considered to be small in the case of the delta wing. Although the arrowhead model is somewhat large for the size of tunnel, it is argued in Ref. 16 that the corrections may be fairly small. The tabulated experimental values are plotted for the arrowhead wing in Fig. 2 and for the delta wing in Fig. 4. Each value of m_θ lies very close to the present theoretical curve against pitching axis. The comparison of theoretical and experimental values of z_θ is fair for the arrowhead wing and good for the delta wing.

Since the present theory neglects terms of order ω^2, it is encouraging to find experimentally that the effects of frequency are small and that the values of the pitching derivatives are reasonably close to those calculated theoretically. The variation in m_θ with both pitching axis and aspect ratio in Fig. 4 is very consistent and demonstrates the practical importance of the theory at low speeds. The curves of m_θ against Mach number in Fig. 8 are in fair agreement. For the pitching axis $x_0 = 0{\cdot}973\bar{c}$, the experimental variation in m_θ $(0{\cdot}4 < M < 0{\cdot}9)$ is about 67 per cent of the theoretical. In the case $x_0 = 0{\cdot}754\bar{c}$, the measured $-m_\theta$ is some 20 per cent below theory and changes rather less at lower Mach numbers. However a much steeper rise where $M > 0{\cdot}8$ brings the total experimental variation $(0{\cdot}4 < M < 0{\cdot}9)$ up to 90 per cent of the theoretical.

10. *Concluding Remarks.*—(*a*) *Description of Method.*—This report describes an extension of Multhopp's subsonic lifting-surface theory (Ref. 1) from steady flow to harmonic pitching oscillations of low frequency (sections 2 to 5) and its application to wings of circular, arrowhead and delta plan-forms (section 6). In equations (78) and (79) the pitching derivatives m_θ and z_θ are expressed in terms of the steady theory with changed boundary conditions.

Full details of the general computation are given in Appendix II, which should be studied in conjunction with Appendix VII of Ref. 1. With the aid of tables of four influence functions (Ref. 11), obtainable from the Aerodynamics Division, N.P.L., the procedure becomes straightforward. The stages of calculation are set out at the end of section 5. At the outset a single parameter m, defining the pivotal spanwise stations, must be chosen. Once m is fixed the computation is specific.

(*b*) *Salient Results.*—Three very different plan-forms have been calculated for two values of m. Each gives reasonably consistent values of the pitching derivatives (section 6.1).

Numerical results are discussed in relation to the corresponding derivatives z_q and m_q of a uniform pitching rotation (section 7.2), thus evaluating the deficiencies of a purely steady theory (section 7.1) for oscillatory derivatives. These deficiencies apparently grow with decreasing aspect ratio : in practice the damping of pitching oscillations can be expected to be greater than the derivative m_q would suggest. Steady pitching ceases to be a useful guide when the effects of compressibility are important.

For delta wings the theoretical effects of aspect ratio are found to be small (section 6.2). Compressibility, however, has a large theoretical effect, which, for delta wings, usually tends towards greater stability (section 6.3) and is surprisingly sensitive to pitching axis (Fig. 7).

The damping of pitching oscillations about the calculated aerodynamic centre is plotted against sweepback in Fig. 9. For incompressible flow the points for the five wings lie on a common curve : the large effect of Mach number is indicated.

(*c*) *Summarized Comparisons.*—Since the theory neglects all terms involving the square of the frequency ω, it is encouraging to find that the experimental derivatives show no marked effect of frequency at the highest available values of the parameter $\omega\bar{c}/U$ (section 9). The practical significance of the theory is borne out by experimental evidence up to a Mach number of about $0{\cdot}9$ (Figs. 4 and 8), though the theory is not strictly valid when shock-waves are present.

Low aspect ratio theory (Appendix III) for cropped delta wings approximates to numerical results in incompressible flow at very low aspect ratios (Figs. 6 and 7), but is generally unsuitable. Inconsistent derivatives for the oscillating circular plate are found in Refs. 7 and 8 (section 8.1).

Calculations from Ref. 5 agree fairly well with the present results for circular, arrowhead and delta wings (section 8.2). From comparisons with Ref. 5 and experiment it seems that the uncertainty in stability derivatives for slow pitching has been greatly reduced.

(*d*) *Limitations of Theory.*—The present theory is valid provided that $\omega\bar{c}M/U(1 - M^2)$ is small compared with unity ; the method is thus inapplicable to practical values of ω at very high subsonic speeds. It remains to be seen to what extent these considerations are masked by the interference of shock-waves.

In incompressible flow the integral equation (37) is valid for all frequencies. It follows from Appendix I that the complex downwash $\bar{w} = \bar{w}_1 + i\bar{w}_2$ neglects complex terms in ω^2 and a real term

$$\frac{\Delta \bar{w}_1}{U} = \frac{S\bar{C}_L}{16\pi U^2}\omega^2 \log\frac{\omega\bar{c}}{U} = \frac{A\bar{C}_L}{16\pi}\left(\frac{\omega\bar{c}}{U}\right)^2 \log\frac{\omega\bar{c}}{U}\,.$$

When $\omega\bar{c}/U = 1/\sqrt{\mathrm{e}} = 0\cdot61$, the magnitude of this uniform induced incidence has a maximum. Its ratio to the amplitude of oscillations is then

$$\frac{A}{32\pi\mathrm{e}}\,(C_L)_1\,,$$

which for the delta wing ($A = 3$) with $(C_L)_1 = 3\cdot05$, only amounts to a correction of $3\cdot3$ per cent to the lift in phase with the pitching motion. The error in the out-of-phase derivatives ($\omega \to 0$) is of similar order ω^2.

The limitations imposed by assuming only two terms in the chordwise loading in equation (42) cannot be evaluated at this stage, but will presumably become important if the aspect ratio is small enough. Errors from this source would become apparent from calculations with three chordwise terms and three boundary conditions at each pivotal station. The theory is easily generalized in this way, but the calculations require two further influence functions.

Two limitations of the theory arise from complications in the evaluation of downwash (section 6.1) :

(1) logarithmic singularity in the spanwise integral ;

(2) divergent integral at a 'kinked' section.

Both of these are treated by devices dependent on the choice of m. Device (1) is not wholly satisfactory for pointed wings. Device (2) is thought to be the main cause of the fairly small discrepancies that occur for the arrowhead and delta wings with change of m.

A practical limitation is the labour of computation for wings of high aspect ratio at low Mach numbers. Given a new swept plan-form, the work on a desk calculator would run to 7 weeks, when $\beta A > 5$, compared with 4 days when $\beta A < 2$ (section 6.2).

(*e*) *Further Theoretical Work.*—(i) The effect of frequency may become important at high subsonic Mach numbers ; this might be investigated on the basis of Ref. 17 by using the vortex-lattice technique of Ref. 4.

(ii) Multhopp's theory, steady and unsteady, has been generalized to include three chordwise terms ; some calculations for a delta wing are in progress.

(iii) It is desirable to develop methods of cutting down the length of computations when m is large.

(iv) The theory is readily extended to the problem of oscillating control surfaces, and it could estimate some much needed derivatives.

(v) The oscillating circular plate has been treated independently in Refs. 7 and 8. Inconsistent results suggest that the complicated analysis in both of these methods should be checked.

(vi) It is intended to apply Multhopp's theory to calculate pitching derivatives of rectangular and triangular wings of low aspect ratio, thus providing interesting comparisons with the theories of Refs. 9 and 10.

11. *Acknowledgement.*—Most of the numerical results given in this report were calculated by Miss J. S. Francis of the Aerodynamics Division, N.P.L.

12. *Nomenclature.*

a		Speed of sound
$a_{\nu n}$		Coefficients for approximate integration in (55)
A		Aspect ratio ($= 4s^2/S$)
$b_{\nu n}$, $b_{\nu\nu}$		Coefficients for approximate integration in (24)
$c(y)$; $\bar{c}$		Local wing chord ; mean chord ($= S/2s$)
c_r ; c_t		Root chord ($\eta = 0$) ; tip chord ($\eta = 1$)
C_L		Lift coefficient ($= L/\frac{1}{2}\rho U^2 S$)
C_m		Pitching-moment coefficient ($= \mathcal{M}/\frac{1}{2}\rho U^2 S\bar{c}$)
$(C_m)_0$	=	$C_m + C_L x_0/\bar{c}$ (about pitching axis)
i	=	$\sqrt{(-1)}$: influence function corresponding to γ in (44)
ii, jj		Influence functions in (46)
$\overline{i_{\nu\nu}}$, $\overline{j_{\nu\nu}}$, etc.		Influence coefficients in (54) (*see* also Appendix II and Ref. 13)
I ; $\bar{I}$		Enthalpy per unit volume ; its complex amplitude in (8)
I_L, I_m		Lift, pitching-moment contributions for 'equivalent wing' in (74)
I_m^*		Particular value of I_m in (75)
j		Influence function corresponding to μ in (44)
l ; $\bar{l}$		Non-dimensional wing loading ($= \Delta p/\frac{1}{2}\rho U^2$) ; its complex amplitude
m		Number of wing sections taken into account
m_q		Rotary derivative of pitching moment in (87) [$= \frac{1}{2}\partial(C_m)_0/\partial(q\bar{c}/U)$]
$m_{\dot\theta}$		Oscillatory derivative of pitching moment in (79) [$= \frac{1}{2}\partial(C_m)_0/\partial(\dot\theta\bar{c}/U)$]
M		Mach number ($= U/a$)
$\mathcal{M}$		Pitching moment about axis $x = 0$
p ; Δp		Pressure ; lift per unit area
q		Steady rate of pitching
Q		Amplitude of pitching oscillation
(R, ψ)		Polar co-ordinates for influence functions in (35)

s		Semi-span of wing
S		Surface area of wing
t		Time
U		Velocity of undisturbed flow relative to wing
(u, v, w)		Additional velocities in x, y, z, directions
$\bar{w}$	=	$\bar{w}_1 + i\bar{w}_2$. Complex amplitude of w in (16) and (39)
x		Rectangular co-ordinate in U direction from leading edge of central section
(x', y')		Co-ordinates at inducing station ($\eta = \eta_n$)
x_0		Position of pitching axis : variable of integration (18)
x_l ; x_{nl}		Position of leading edge ; value at $\eta = \eta_n$
X		Co-ordinate for influence functions $[= (x - x_l')/c(y')]$
y		Rectangular co-ordinate to starboard from plane of symmetry
Y		Co-ordinate for influence functions $[= \sqrt{(1 - M^2)}(y - y')/c(y')]$
z		Rectangular co-ordinate upwards : equation of wing surface
z_q		Rotary derivative of lift in (86) $[= - \frac{1}{2}\partial C_L/\partial(q\bar{c}/U)]$
$z_{\dot{\theta}}$		Oscillatory derivative of lift in (78) $[= - \frac{1}{2}\partial C_L/(\dot{\theta}\bar{c}/U)]$
α		Local incidence of wing $(= - \partial z/\partial x)$
α_1	=	1 (uniform incidence)
α_2	=	$x/\bar{c}$ (steady pitching)
α_3		Induced incidence in (64)
β		Factor for compressibility $[= \sqrt{(1 - M^2)}]$
γ ; $\bar{\gamma}$		Non-dimensional local lift ; its complex amplitude in (42)
η, η'		Spanwise co-ordinates $(= y/s, y'/s)$
η_n		η at inducing station $\{ = \sin n\pi/(m + 1)\}$ $[- \frac{1}{2}(m - 1) \leqslant n \leqslant \frac{1}{2}(m - 1)]$
η_ν		η at pivotal station $\{= \sin \nu\pi/(m + 1)\}$ $[- \frac{1}{2}(m - 1) \leqslant \nu \leqslant \frac{1}{2}(m - 1)]$
$\dot{\theta}$		Rate of pitching $(= \partial\alpha/\partial t)$
λ		Taper ratio $(= c_t/c_r)$: parameter in (8) and (9)
$\mu, \bar{\mu}$		Non-dimensional local pitching moment in (21), (42)
ρ		Density
ϕ		Angular chordwise co-ordinate in (21)
ω		Frequency of pitching oscillation
$_\infty$		Suffix denoting undisturbed flow
$_{n, \nu}$		Suffixes numerating the spanwise stations η_n, η_ν
$_{\nu n}$		Double suffix numerating X, Y, i, j, etc.
$_{1, 2, 3}$		Suffixes specifying $\bar{\gamma}$, $\bar{\mu}$, $\bar{l}$, I_L, I_m corresponding to α_1, α_2, α_3
$'$		Single stroke denoting x_ν' $(0\cdot9045c)$ in (29)
$''$		Double stroke denoting x_ν'' $(0\cdot3455c)$ in (29)
$\sum\limits_{-\frac{1}{2}(m-1)}^{\frac{1}{2}(m-1)}{}'$		Summation in n with $n = \nu$ omitted.

REFERENCES

No.	*Author*	*Title, etc.*
1	H. Multhopp	Methods for calculating the lift distribution of wings. (Subsonic lifting-surface theory.) R. & M. 2884. January, 1950.
2	W. P. Jones	The calculation of aerodynamic derivative coefficients for wings of any plan-form in non-uniform motion. R. & M. 2470. December, 1946.
3	V. M. Falkner	The calculation of aerodynamic loading on surfaces of any shape. R. & M. 1910. August, 1943.
4	D. E. Lehrian	Aerodynamic coefficients for an oscillating delta wing. R. & M. 2841. July, 1951.
5	D. E. Lehrian	Calculation of stability derivatives for oscillating wings. R. & M. 2922. February, 1953.
6	H. C. Garner	Swept-wing loading. A critical comparison of four subsonic vortex sheet theories. C.P.102. July, 1951.
7	T. Schade and K. Krienes	The oscillating circular aerofoil on the basis of potential theory. N.A.C.A. Tech. Memo. 1098. February, 1947.
8	N. E. Kochin	Steady vibrations of wing of circular plan form. N.A.C.A. Tech. Memo. 1324. Part I. January, 1953.
9	E. Reissner	The effect of finite span on the airload distributions for oscillating wings. I—Aerodynamic theory of the oscillating wing of finite span. N.A.C.A. Tech. Note 1194. March, 1947.
10	H. R. Lawrence and E. H. Gerber	The aerodynamic forces on low aspect ratio wings oscillating in an incompressible flow. Cornell Aeronautical Laboratory, Inc. Report AF–781–A–1. January, 1952. *J. Ae. Sci.* November, 1952.
11	A. R. Curtis	Tables of Multhopp's influence functions. N.P.L. Mathematics Division Report Ma/21/0505. May, 1952.
12	I. E. Garrick	Some research on high-speed flutter. Anglo-American Aeronautical Conference, Brighton, 1951. (Royal Aero. Soc.)
13	K. W. Mangler and B. F. R. Spencer	Some remarks on Multhopp's subsonic lifting-surface theory. R.A.E. Tech. Note Aero. 2181. A.R.C. 15,597. August, 1952. (Unpublished.)
14	G. F. Moss	Low-speed wind-tunnel measurements of longitudinal oscillatory derivatives on three wing plan-forms. R.A.E. Tech. Note Aero. 2208. A.R.C. 15,972. November, 1952.
15	C. Scruton, L. Woodgate and A. J. Alexander.	Measurements of the aerodynamic derivatives for a clipped delta wing of low aspect ratio describing pitching and plunging oscillations in incompressible flow. A.R.C. 15,499. December, 1952. (Unpublished.)
16	C. Scruton, L. Woodgate and A. J. Alexander.	Measurements of the aerodynamic derivatives for arrowhead and delta wings of low aspect ratio describing pitching and plunging oscillations in incompressible flow. R. & M. 2925. October, 1953.
17	W. P. Jones	Oscillating wings in compressible subsonic flow. R. & M. 2855. October, 1951.
18	H. M. Lyon	Aerodynamic derivatives of flexural-torsional flutter of a wing of finite span. R. & M. 1900, Part I. July, 1939.

APPENDIX I

Expansion of Equation (37) in Powers of Frequency

In terms of their amplitudes the downwash and load at a wing are related by the integral equation

$$\bar{w}(x, y) = \frac{U(1-M^2)}{8\pi} \int_{-\infty}^{x} \left\{ \iint_S \frac{\bar{l}(x', y')\, dx'\, dy'}{[(x_0 - x')^2 + (1-M^2)(y-y')^2]^{3/2}} \right\} \exp\left\{ \frac{i\omega(x_0 - x)}{U(1-M^2)} \right\} dx_0 \,. \quad (37)$$

In view of the infinite limit of integration it is not clear whether the exponental term may be expanded in powers of ω to obtain approximations when ω is small. Split the integration into two parts

$$\int_{-\infty}^{x} = \int_{-\infty}^{x-\xi} + \int_{x-\xi}^{x}$$

such that $x' > (x - \xi)$ throughout the plan-form S. Then it is valid to expand

$$\exp\{i\omega(x_0 - x)/U(1-M^2)\} = 1 + \frac{i\omega(x_0 - x)}{U(1-M^2)} - \frac{\omega^2(x_0-x)^2}{2U^2(1-M^2)^2} + \ldots$$

under the integral sign for the part $\int_{x-\xi}^{x}$; and the integrand of $\iint_S$ for the range $x_0 < (x - \xi)$ has no singularity. If $-\xi$ is large enough, the lengths $(x - x')$ and $\sqrt{(1-M^2)}(y - y')$ in the denominator become secondary compared with $(x_0 - x)$; then asymptotically

$$\iint_S \frac{\bar{l}(x', y')\, dx'\, dy'}{[(x_0 - x')^2 + (1-M^2)(y-y')^2]^{3/2}} \sim \iint_S \frac{\bar{l}(x', y')}{(x - x_0)^3}\, dx'\, dy' \sim S\bar{C}_L/(x - x_0)^3,$$

where $\bar{C}_L$ is the amplitude of the lift coefficient. The part $\int_{-\infty}^{x-\xi}$ contributes to $\bar{w}(x, y)$ an amount

$$\frac{U(1-M^2)}{8\pi} \int_{-\infty}^{x-\xi} \frac{S\bar{C}_L}{(x-x_0)^3} \exp\{i\omega(x_0 - x)/U(1-M^2)\}\, dx_0 + \text{secondary terms}$$

$$= \frac{U(1-M^2)S\bar{C}_L}{8\pi} \int_{\xi}^{\infty} \xi^{-3} \exp(-i\lambda\xi) \,,$$

where $\lambda = \omega/U(1-M^2)$. The expansion of this integral follows from Miss Lyon's analysis in Appendix I, equation (87) of Ref. 18 (1939) :

$$\int_{\xi}^{\infty} \xi^{-3} \exp(-i\lambda\xi)\, d\xi = -\left[\left(\frac{1}{2\xi^2} - \frac{i\lambda}{2\xi}\right) \exp(-i\lambda\xi)\right]_{\xi}^{\infty} - \tfrac{1}{2}\lambda^2 \int_{\xi}^{\infty} \xi^{-1} \exp(-i\lambda\xi)\, d\xi$$

$$= \frac{1}{2\xi^2} - \frac{i\lambda}{\xi} - \tfrac{1}{2}\lambda^2 [\tfrac{3}{2} - \gamma - \log \lambda\xi - \tfrac{1}{2}i\pi] + \ldots,$$

where γ is Euler's constant. Thus the contribution to $\bar{w}(x, y)$ of the part $\int_{-\infty}^{x-\xi}$ includes a real term

$$\frac{S\bar{C}_L\omega^2}{16\pi U(1-M^2)} \log \frac{\omega\bar{c}}{U(1-M^2)} \,,$$

which is independent of ξ. This shows that the exponential may not be expanded under the integral sign for the part $\int_{-\infty}^{x-\xi}$ beyond the term in ω. But since there is no term in $\omega \log \omega$, the original integral (37) may be replaced by

$$\bar{w}(x, y) = \frac{U(1-M^2)}{8\pi} \int_{-\infty}^{x} \left\{ \iint_S \frac{\bar{l}(x', y')\, dx'\, dy'}{[(x_0 - x')^2 + (1-M^2)(y-y')^2]^{3/2}} \right\} \left\{ 1 + \frac{i\omega(x_0 - x)}{U(1-M^2)} \right\} dx_0$$

to the first order in frequency.

APPENDIX II

Instructions for Computers

To anyone familar with Multhopp's steady subsonic lifting-surface theory its extension to harmonic pitching oscillations of low frequency should present little difficulty. A reader without any experience of the steady theory should first study Appendix VII of Ref. 1 with the help of the worked examples.

Pitching oscillations require the use of two chordwise pivotal points and are associated with symmetrical loading. The procedure to be followed therefore closely resembles that given in pages 55 to 59 of Ref. 1 and illustrated in Tables 13 to 22. The stages of the calculation will now be described.

(*a*) *Choice of m.*—At the outset of a calculation the number of spanwise stations has to be determined. The essential constants for $m = 3, 5, 7, 11, 15, 23, 31$ are collected in Tables 1 to 7 of Ref. 1. The condition $m > 3A\beta$ gives an approximate critical table

$A\beta$	0		1		1·5		2·5		3·5		5		7·5		10
m		3		5		7		11		15		23		31	

Thus, when $1 < A\beta < 1{\cdot}5$, $m = 5$ is recommended provided that the contour of the wing is fairly smooth. It is, however, unwise to use $m < 7$, if the leading edge of the wing is highly swept ($> \tan^{-1}\beta$) with a central kink ; and for such wings $m = 7$ is suggested for the whole range $0 < A\beta < 2{\cdot}5$.

(*b*) *Functions of One Variable.*—The first calculations involve symmetrical functions of a single variable ν or n, $|\nu|$ or $|n|$ taking the values $0, 1, 2, \ldots \frac{1}{2}(m-1)$. These should be arranged in a form similar to Table 13 of Ref. 1 and subdivided into four sections, associated with

(i) wing geometry,

(ii) steady solution,

(iii) evaluation of α_3,

(iv) evaluation of pitching moments.

When compressibility is taken into account, it is convenient to work with the 'equivalent wing,' which is specified by the actual plan-form (x_l and c in terms of η) and the 'equivalent' semi-span

$$s\beta = s\sqrt{(1 - M^2)}.$$

In calculating (i) and (ii) the form of Table 13 of Ref. 1 should be followed. But instead of y_ν and $b/2c_n$,

$$\beta y_\nu = s\beta\eta_\nu \text{ and } s\beta/c_n$$

should be calculated ; and then the factor

$$\frac{\eta_{\nu+1} - \eta_{\nu-1}}{m+1} \cos\frac{\nu\pi}{m+1} \cdot \left(\frac{s\beta}{c_\nu}\right)^2 ,$$

from which $\overline{i_{\nu\nu}}'$, $\overline{j_{\nu\nu}}'$, $\overline{i_{\nu\nu}}''$, $\overline{j_{\nu\nu}}''$ may be evaluated from equations (54). The evaluation of l_ν', l_ν'', m_ν'', m_ν' in equations (30) then completes (ii).

Section (iii) contains five quantities :

four additional influence functions $\overline{ii_{\nu\nu}}'$, $\overline{jj_{\nu\nu}}'$, $\overline{ii_{\nu\nu}}''$, $\overline{jj_{\nu\nu}}''$, which are calculated from equations (54) similarly to $\overline{i_{\nu\nu}}'$, etc., and $c_n/\bar{c}$,

$$\text{where } \bar{c} = \frac{\text{wing area}}{\text{wing span}} = \frac{2s}{A} .$$

Section (iv) involves four parameters which occur in the expressions for $(I_m)_1$ and $I_m{}^*$ in equations (73) and (75) :

$$c_n/s\beta \, , \qquad (x_{nl} + 0\cdot25c_n)/s\beta ,$$

$$\frac{2x_{nl}c_n + 0\cdot75c_n{}^2}{\bar{c}\, .\, s\beta} \, , \qquad \frac{x_{nl}{}^2 + 0\cdot5x_{nl}c_n + 0\cdot125c_n{}^2}{\bar{c}\, .\, s\beta} .$$

The last two of these are only used in compressible flow.

(*c*) *Formulation of Equations.*—The procedure in Ref. 1 is set out in Tables 14 to 17 for an example in which $m = 15$. The essential difference now is that the influence functions are being determined from tables (Ref. 11) instead of charts (Ref. 1, Figs. 1 to 6).

A separate table is required for each value of $|n|$, taking positive and negative values such that $|\nu - n|$ is odd. Instead of $|Y_{\nu n}|$, $X_{\nu n}'$, $X_{\nu n}''$, it is necessary to calculate

$$|2Y_{\nu n}| = 2\frac{s\beta}{c_n}\,|\eta_\nu - \eta_n| ,$$

$$2X_{\nu n}' - 1 = \frac{2x_\nu' - 2x_{nl}}{c_n} - 1 ,$$

$$2X_{\nu n}'' - 1 = \frac{2x_\nu'' - 2x_{nl}}{c_n} - 1 ;$$

and then

$$R_{\nu n}' = \sqrt{\{|2Y_{\nu n}|^2 + (2X_{\nu n}' - 1)^2\}} \text{ or } 1/R_{\nu n}', \text{ if } R_{\nu n}' > 2 ,$$

$$\psi_{\nu n}' = \cos^{-1}\{(2X_{\nu n}' - 1)/R_{\nu n}'\} \qquad (0 \text{ deg} < \psi_{\nu n}' < 180 \text{ deg}) ;$$

and similarly $R_{\nu n}''$, $\psi_{\nu n}''$ and $1/R_{\nu n}''$ (if required). $\psi_{\nu n}'$ and $\psi_{\nu n}''$ should be expressed in degrees and decimals.

Then $i_{\nu n}'$, $j_{\nu n}'$ and $i_{\nu n}''$, $j_{\nu n}''$ are evaluated by interpolation in Ref. 11, where the influence functions are tabulated for $\psi = 0$ deg (1 deg) 180 deg in the two regions $R = 0\cdot20(0\cdot05)2\cdot00$ and $1/R = 0\cdot00(0\cdot05)0\cdot50$. The four quantities

$$a_{\nu n}(l_\nu' i_{\nu n}' - l_\nu'' i_{\nu n}'')$$

$$a_{\nu n}(l_\nu' j_{\nu n}' - l_\nu'' j_{\nu n}'')$$

$$a_{\nu n}(m_\nu'' i_{\nu n}'' - m_\nu' i_{\nu n}')$$

$$a_{\nu n}(m_\nu'' j_{\nu n}'' - m_\nu' j_{\nu n}')$$

are then determined as in Tables 14 to 17 of Ref. 1, the values of $a_{\nu n}$ being given in Tables 1 to 7 for the appropriate value of m.

Hence the $2m$ linear equations (30) are formed and will determine the $2m$ unknowns γ_n and μ_n for any set of values of the incidences α_ν' and α_ν''.

(*d*) *Solution of Equations*.—In view of the symmetry, $\gamma_n = \gamma_{-n}$ and $\mu_n = \mu_{-n}$, the equations reduce to a set of order $(m + 1)$. This reduction is achieved by the formulae on page 57 of Ref. 1, the values of the coefficients $B_{\nu n}$, $C_{\nu n}$, $D_{\nu n}$, $E_{\nu n}$, being entered separately for even and odd values of n, as in Tables 18(a) and 19(a) respectively.

The problem of slow pitching oscillations introduces three sets of incidences,

$$\left.\begin{aligned} \alpha &= \alpha_1 = 1 \text{ (everywhere)} \\ \alpha &= \alpha_2 = x/\bar{c}, \text{ i.e., } (\alpha_\nu')_2 = x_\nu'/\bar{c} \\ &\qquad\qquad\qquad\quad (\alpha_\nu'')_2 = x_\nu''/\bar{c} \\ \alpha &= \alpha_3 \text{ (to be calculated)} \end{aligned}\right\} .$$

The terms

$$a_{\nu\nu}(l_\nu'\ \alpha_\nu' - l_\nu''\ \alpha_\nu'')$$
$$a_{\nu\nu}(m_\nu''\ \alpha_\nu'' - m_\nu'\ \alpha_\nu')$$

are then calculated for a set of incidences ; and the iterative solution is then carried out by the process fully described and illustrated on pages 58 and 59 and Tables 18 to 21 of Ref. 1. Hence the values

$(\gamma_n)_1$, $(\mu_n)_1$ corresponding to α_1

$(\gamma_n)_2$, $(\mu_n)_2$ corresponding to α_2

$(\gamma_n)_3$, $(\mu_n)_3$ corresponding to α_3

are determined to the desired accuracy.

(*e*) *Calculation of* α_3.

From equation (64),

$$\frac{(\alpha_\nu)_3}{b_{\nu\nu}} \cdot \bar{c} = \{\overline{ii}_{\nu\nu}\,(\gamma_\nu)_1 c_\nu + \overline{jj}_{\nu\nu}(\mu_\nu)_1 c_\nu\} - \sum_{-\frac{1}{2}(m-1)}^{\frac{1}{2}(m-1)}{}' \ a_{\nu n}\{ii_{\nu n}(\gamma_n)_1 c_n + jj_{\nu n}(\mu_n)_1 c_n\} .$$

First the influence functions $ii_{\nu n}'$, $jj_{\nu n}'$ and $ii_{\nu n}''$, $jj_{\nu n}''$ are evaluated by interpolation in the tables of Ref. 11. Then

$$f_{\nu n}' = a_{\nu n}\{ii_{\nu n}'(\gamma_n)_1 + jj_{\nu n}'(\mu_n)_1\}$$
$$f_{\nu n}'' = a_{\nu n}\{ii_{\nu n}''(\gamma_n)_1 + jj_{\nu n}''(\mu_n)_1\}$$

are evaluated for each (ν, n) such that $|\ \nu - n\ |$ is odd, $(\gamma_n)_1$ and $(\mu_n)_1$ being already obtained for a unit incidence. Then for each ν the values of

$$f_{\nu\nu}' = \overline{ii}_{\nu\nu}'(\gamma_\nu)_1 + \overline{jj}_{\nu\nu}'(\mu_\nu)_1$$
$$f_{\nu\nu}'' = \overline{ii}_{\nu\nu}''(\gamma_\nu)_1 + \overline{jj}_{\nu\nu}''(\mu_\nu)_1$$

are listed, $\overline{ii}_{\nu\nu}'$, etc., being taken from the first sheet of calculations. Finally since $a_{\nu\nu} = 1/b_{\nu\nu}$,

$$\left.\begin{aligned} a_{\nu\nu}(\alpha_\nu')_3 &= f_{\nu\nu}' \cdot c_\nu/\bar{c} - \sum_{-\frac{1}{2}(m-1)}^{\frac{1}{2}(m-1)}{}' f_{\nu n}'\ c_n/\bar{c} \\ a_{\nu\nu}(\alpha_\nu'')_3 &= f_{\nu\nu}''\ c_\nu/\bar{c} - \sum_{-\frac{1}{2}(m-1)}^{\frac{1}{2}(m-1)}{}' f_{\nu n}''\ c_n/\bar{c} \end{aligned}\right\} ,$$

where the summations in n omit $n = \nu$ and the values of $c_n/\bar{c}$ are taken from the first sheet of calculations.

(*f*) *Evaluation of Influence Functions.*—The tables of Ref. 11 are constructed to give the values of i, j, ii, jj within about $\pm 0\cdot 0001$ for the practical range of the polar co-ordinates (R, ψ). Equations (30) show that the solution demands a certain accuracy in $a_{\nu n} i_{\nu n}$, etc., where from equation (55)

$$a_{\nu n} = \frac{4 \cos \dfrac{\nu\pi}{m+1} \cos \dfrac{n\pi}{m+1}}{(m+1)^2 (\eta_\nu - \eta_n)^2} < \frac{4}{(m+1)^2} \cot^2 \frac{|\nu - n|\pi}{2(m+1)} .$$

The greatest accuracy in the influence functions is required when $|\nu - n| = 1$. It follows that requirements in accuracy for the other values of $|\nu - n|$ can be relaxed in the inverse ratio of $a_{\nu n}$. Thus $i_{\nu n}, j_{\nu n}, ii_{\nu n}, jj_{\nu n}$ are only required within

$$\pm\, 0\cdot 0001 \left(\tan \frac{|\nu - n|\pi}{2(m+1)} \bigg/ \tan \frac{\pi}{2(m+1)} \right)^2$$

or

$$\pm\, 0\cdot 0001\ (\nu - n)^2.$$

A. R. Curtis of the Mathematics Division, N.P.L., has shown that the four influence functions are related by the formula

$$i(R^2 + 2X) + j \,.\, \tfrac{1}{4}(2X - 1) - ii\{2(2X - 1) + 1\} - jj \,.\, \tfrac{3}{4} = (2Y)^2.$$

This equation constitutes a very useful check on the calculations after the evaluation of $(2X - 1)$ and $2Y$, which are themselves conveniently sum-checked. Although the formula will not check jj to great accuracy, when $(R^2 + 2X)$ is large, it will normally provide a check to the required accuracy of $\pm 0\cdot 0001(\nu - n)^2$, provided that i has been obtained to the greatest accuracy (of about $\pm 0\cdot 0001$). The use of such a check is strongly recommended; and it is desirable to complete the evaluation of all four influence functions for this purpose before proceeding with the other stages of the calculation.

(*g*) *Oscillatory Pitching Derivatives.*—Once the equations have been solved for the three incidences α_1, α_2, α_3, the pitching derivatives are easily determined by seven coefficients

$$(I_L)_1 = \frac{\pi}{m+1} (A\beta) \sum_{-\frac{1}{2}(m-1)}^{\frac{1}{2}(m-1)} (\gamma_n)_1 \cos \frac{n\pi}{m+1}$$

$$(I_m)_1 = \frac{\pi}{2(m+1)} (A\beta)^2 \sum_{-\frac{1}{2}(m-1)}^{\frac{1}{2}(m-1)} \left\{ (\mu_n)_1 c_n/s\beta - (\gamma_n)_1 (x_{nl} + 0\cdot 25 c_n)/s\beta \right\} \cos \frac{n\pi}{m+1}$$

$$I_m{}^* = \frac{\pi}{2(m+1)} (A\beta)^2 \sum_{-\frac{1}{2}(m-1)}^{\frac{1}{2}(m-1)} \left((\mu_n)_1 \frac{2x_{nl}c_n + 0\cdot 75 c_n{}^2}{\bar{c} \,.\, s\beta} \right.$$

$$\left. - (\gamma_n)_1 \frac{x_{nl}{}^2 + 0\cdot 5 x_{nl} c_n + 0\cdot 125 c_n{}^2}{\bar{c} \,.\, s\beta} \right) \cos \frac{n\pi}{m+1} ,$$

and $(I_L)_2$, $(I_m)_2$, $(I_L)_3$, $(I_m)_3$, given similarly to $(I_L)_1$, $(I_m)_1$. These are evaluated on the lines of Table 22 of Ref. 1 by using the functions of the plan-form tabulated on the first sheet of calculations and values of $\cos \dfrac{n\pi}{m+1} \equiv \sin \theta_n$ given in Tables 1 to 7 of Ref. 1.

Then the pitching derivatives about a pitching axis $x = x_0$ are given by

$$-2z_\theta = \left(-\frac{1-\beta^2}{\beta^3}(I_m)_1 + \frac{2\beta^2-1}{\beta^3}(I_L)_2 + \frac{1}{\beta^3}(I_L)_3\right) - \frac{x_0}{\bar{c}}\frac{1}{\beta}(I_L)_1 ;$$

$$-2m_\theta = \left(-\frac{1-\beta^2}{\beta^3}I_m{}^* - \frac{2\beta^2-1}{\beta^3}(I_m)_2 - \frac{1}{\beta^3}(I_m)_3\right)$$

$$-\frac{x_0}{\bar{c}}\left(-\frac{1}{\beta^3}(I_m)_1 + \frac{2\beta^2-1}{\beta^3}(I_L)_2 + \frac{1}{\beta^3}(I_L)_3\right) + \left(\frac{x_0}{\bar{c}}\right)^2\frac{1}{\beta}(I_L)_1 .$$

(*h*) *General Comments.*—(i) In order to master the principles of the method $(m+1)$ may be chosen to be one-half of its ultimate value. Such preliminary calculations would increase the total labour by only 25 per cent and provide initial guesses for the quantities γ_n, μ_n (n even) in the ultimate solutions by iteration.

(ii) After experience it will be found that some of the writing included in Multhopp's illustrative calculations (Tables 13 to 22 of Ref. 1) can be avoided, particularly in the solutions by iteration.

(iii) When a high-speed computer is available to solve the sets of linear simultaneous equations there is no need to introduce the four quantities l_ν', l_ν'', m_ν'', m_ν' at all. Directly from equation (27) separate conditions

$$\overline{i}_{\nu\nu}\gamma_\nu + \overline{j}_{\nu\nu}\mu_\nu - \sum_{-\frac{1}{2}(m-1)}^{\frac{1}{2}(m-1)}{}' a_{\nu n}(i_{\nu n}\gamma_n + j_{\nu n}\mu_n) = a_{\nu\nu}\alpha_\nu$$

are obtained at the chordwise positions

$$\left.\begin{aligned} x_\nu' &= x_{\nu l} + 0\cdot 9045c_\nu \\ x_\nu'' &= x_{\nu l} + 0\cdot 3455c_\nu \end{aligned}\right\} .$$

With a desk calculator, in fact, an iteration using the separate conditions converges as quickly as the suggested routine in Ref. 1. This method of solution is feasible since $\overline{j}_{\nu\nu}'$ is small compared with $\overline{i}_{\nu\nu}'$, $\overline{i}_{\nu\nu}''$ and $\overline{j}_{\nu\nu}''$. The calculations of successive increments to γ and μ are replaced by direct iterations

$$\gamma_\nu = \frac{1}{\overline{i}_{\nu\nu}'}\left[a_{\nu\nu}\,\alpha_\nu' - \overline{j}_{\nu\nu}'\,\mu_\nu + \sum_{-\frac{1}{2}(m-1)}^{\frac{1}{2}(m-1)}{}' a_{\nu n}(i_{\nu n}'\,\gamma_n + j_{\nu n}'\,\mu_n)\right]$$

$$\mu_\nu = \frac{1}{\overline{j}_{\nu\nu}''}\left[a_{\nu\nu}\,\alpha_\nu'' - \overline{i}_{\nu\nu}''\,\gamma_\nu + \sum_{-\frac{1}{2}(m-1)}^{\frac{1}{2}(m-1)}{}' a_{\nu n}(i_{\nu n}''\,\gamma_n + j_{\nu n}''\,\mu_n)\right] ,$$

an earlier approximation to μ_ν being used in the former equation.

After successive values $\gamma_\nu^{(1)}$, $\gamma_\nu^{(2)}$, $\gamma_\nu^{(3)}$ have been obtained, a better approximation is usually given by

$$\gamma_\nu = \frac{(\gamma_\nu^{(2)})^2 - \gamma_\nu^{(1)}\,.\,\gamma_\nu^{(3)}}{2(\gamma_\nu^{(2)}) - \gamma_\nu^{(1)} - \gamma_\nu^{(3)}} ,$$

if the values themselves are calculated to an extra decimal place. This alternative procedure is recommended once a working facility has been gained.

(iv) If required the steady pitching derivatives, z_q and m_q, may be evaluated from the formulae (86) and (87) in section 7.1. Only the four coefficients $(I_L)_1$, $(I_m)_1$, $(I_L)_2$, $(I_m)_2$ are involved.

(v) Without any increase in computation the approximate formulae (54) for $\overline{i_{\nu\nu}}'$, etc., may be replaced by more rigorous expressions, justified by Mangler and Spencer (Ref. 13) :

at $0 \cdot 9045c$,

$$\left.\begin{aligned} \overline{i_{\nu\nu}}' &= 1\cdot 9742 + 1\cdot 1974\left(\frac{s\beta}{c_\nu}\right)^2 G_\nu \\ \overline{j_{\nu\nu}}' &= 0\cdot 2859 - 9\cdot 2293\left(\frac{s\beta}{c_\nu}\right)^2 G_\nu \\ \overline{ii_{\nu\nu}}' &= 1\cdot 3100 - 0\cdot 2069\left(\frac{s\beta}{c_\nu}\right)^2 G_\nu \\ \overline{jj_{\nu\nu}}' &= 1\cdot 9889 + 2\cdot 1662\left(\frac{s\beta}{c_\nu}\right)^2 G_\nu \end{aligned}\right\}$$

at $0 \cdot 3455c$,

$$\left.\begin{aligned} \overline{i_{\nu\nu}}'' &= 1\cdot 4055 + 1\cdot 9374\left(\frac{s\beta}{c_\nu}\right)^2 G_\nu \\ \overline{j_{\nu\nu}}'' &= 3\cdot 1702 + 11\cdot 0591\left(\frac{s\beta}{c_\nu}\right)^2 G_\nu \\ \overline{ii_{\nu\nu}}'' &= 0\cdot 3323_5 - 0\cdot 8762\left(\frac{s\beta}{c_\nu}\right)^2 G_\nu \\ \overline{jj_{\nu\nu}}'' &= 0\cdot 9780 + 1\cdot 3389\left(\frac{s\beta}{c_\nu}\right)^2 G_\nu \end{aligned}\right\}$$

where for $m = 7$,

ν	0	± 1	± 2	± 3
G_ν	0·04521	0·03831	0·02166	0·00501

for $m = 11$,

ν	0	± 1	± 2	± 3	± 4	± 5
G_ν	0·01961	0·01827	0·01462	0·00963	$0\cdot 00463_5$	$0\cdot 00097_9$

and for $m = 15$,

ν	0	± 1	± 2	± 3	± 4	± 5	± 6	± 7
G_ν	0·01094	0·01052	0·00932	0·00753	$0\cdot 00541_5$	0·00330	$0\cdot 00150_7$	$0\cdot 00030_9$

All the present calculations are based on the formulae (54).

APPENDIX III

Low Aspect Ratio Theory

In reviewing some research on flutter[12] (1951), Garrick has included analytical results for unsteady incompressible flow past wings of very small aspect ratio by generalizing the classical steady theory of R. T. Jones.

The upward component of velocity at the surface satisfies

$$\begin{aligned} w &= \frac{\partial z}{\partial t} + U\frac{\partial z}{\partial x} \\ &= -\,QU\cos\omega t + Q\omega(x - x_0)\sin\omega t\,, \end{aligned}$$

as in equation (59) of section 5. Then, if $2s(x)$ denotes the span of a transverse strip of the wing, the lift per unit length in the direction of the stream is given by equation (6) of Appendix B to Ref. 12 as follows :

$$\begin{aligned} l(s) &= -\,\pi\rho s^2\left(\frac{\partial^2 z}{\partial t^2} + 2U\frac{\partial^2 z}{\partial x\partial t} + U^2\frac{\partial^2 z}{\partial x^2}\right) - 2\pi\rho U s\frac{ds}{dx}\left(\frac{\partial z}{\partial t} + U\frac{\partial z}{\partial x}\right) \\ &= -\,\pi\rho s^2\left(\frac{\partial w}{\partial t} + U\frac{\partial w}{\partial x}\right) - 2\pi\rho U s\frac{ds}{dx}\,w \\ &= \pi\rho s Q\left[\left(2U^2\frac{ds}{dx} - \omega^2 s(x - x_0)\right)\cos\omega t - 2U\omega\left(s + \frac{ds}{dx}(x - x_0)\right)\sin\omega t\right]. \end{aligned}$$

From equation (58), $\dot\theta = -\,\omega Q\sin\omega t.$

Then out of phase with the pitching motion

$$l(x) = 2\pi\rho U s\dot\theta\left(s + \frac{ds}{dx}(x - x_0)\right),$$

where $s = s(x)$. For a delta wing of taper ratio $\lambda = 1/7$

$$\left.\begin{aligned} s &= \tfrac{1}{3}Ax \text{ for } 0 < x < \tfrac{3}{2}\bar c \\ &= \tfrac{1}{2}A\bar c \text{ for } \tfrac{3}{2}\bar c < x < \tfrac{7}{4}\bar c \end{aligned}\right\}.$$

Thus

$$\left.\begin{aligned} l(x) &= \tfrac{2}{9}\pi\rho A^2U\dot\theta\,\{x^2 + x(x - x_0)\} \text{ for } 0 < x < \tfrac{3}{2}\bar c \\ &= \tfrac{1}{2}\pi\rho A^2U\dot\theta\bar c^2 \qquad\qquad \text{for } \tfrac{3}{2}\bar c < x < \tfrac{7}{4}\bar c \end{aligned}\right\}.$$

Then

$$\begin{aligned} C_L &= \int_0^{7\bar c/4} l(x)\,dx/\tfrac{1}{2}\rho U^2 S, \text{ where } S = A\bar c^2\,, \\ &= \frac{2\pi A\dot\theta}{U\bar c^2}\left[\tfrac{2}{9}(\tfrac{9}{4}\bar c^3 - \tfrac{9}{8}x_0\bar c^2) + \tfrac{1}{2}\bar c^2\,.\,\tfrac{1}{4}\bar c\right] = 2\pi A\frac{\dot\theta\bar c}{U}(\tfrac{5}{8} - \tfrac{1}{4}x_0/\bar c)\,. \end{aligned}$$

$$\begin{aligned} (C_m)_0 &= \int_0^{7\bar c/4} l(x)(x_0 - x)\,dx/\tfrac{1}{2}\rho U^2 S\bar c \\ &= \frac{x_0}{\bar c}C_L - \frac{2\pi A\dot\theta}{U\bar c^3}\left[\tfrac{2}{9}(\tfrac{81}{32}\bar c^4 - \tfrac{9}{8}x_0\bar c^3) + \tfrac{1}{2}\bar c^2\,\tfrac{13}{32}\bar c^2\right]. \\ &= -\,2\pi A\frac{\dot\theta\bar c}{U}\left[\tfrac{49}{64} - \tfrac{7}{8}(x_0/\bar c) + \tfrac{1}{4}(x_0/\bar c)^2\right], \end{aligned}$$

Thus the derivatives, defined in equations (78) and (79), are

$$\left.\begin{aligned} z_{\dot\theta} &= -\,\tfrac{1}{2}\partial C_L/\partial\left(\frac{\dot\theta\bar c}{U}\right) = -\,\pi A\left(\tfrac{5}{8} - \tfrac{1}{4}(x_0/\bar c)\right) \\ m_{\dot\theta} &= \tfrac{1}{2}\partial(C_m)_0/\partial\left(\frac{\dot\theta\bar c}{U}\right) = -\,\pi A\left(\tfrac{7}{8} - \tfrac{1}{2}(x_0/\bar c)\right)^2 \end{aligned}\right\}.$$

$-\,m_{\dot\theta}$ has a minimum value of zero about the trailing edge $x_0 = 1{\cdot}75\bar c$.

It is clear from Fig. 4 that even for aspect ratios as low as 2 or 1·2, neither $z_{\dot\theta}$ nor $m_{\dot\theta}$ is approximately proportional to A. But when $A < \frac{1}{2}$, these formulae are apparently more consistent with the numerical results of Multhopp's theory plotted in Figs. 6 and 7.

TABLE 1

Summary of Coefficients for Pitching Derivatives

Wing	A	Solution	$(I_L)_1$	$(I_L)_2$	$(I_L)_3$	$I_L^* = -(I_m)_1$	$-(I_m)_2$	$-(I_m)_3$	$-I_m^*$
Circle	$4/\pi$	$m = 7$	1·788	1·736	0·954	0·541	0·901	0·629	0·268
Circle	$4/\pi$	$m = 5$	1·793	1·746	0·974	0·539	0·906	0·634	0·265
Arrowhead	1·32	$m = 11$	1·644	2·482	0·610	1·622	2·758	0·696	1·860
Arrowhead	1·32	$m = 5$	1·704	2·571	0·717	1·615	2·792	0·812	1·779
Delta	3	$m = 15$	3·050	4·601	0·491	2·845	4·816	0·622	3·159
Delta	3	$m = 7$	3·071	4·592	0·602	2·820	4·754	0·681	3·092
Delta	2	$m = 7$	2·387	3·660	0·821	2·250	3·911	0·933	2·496
Delta	1·2	$m = 7$	1·624	2·563	0·762	1·594	2·854	0·885	1·807

TABLE 2

Pitching Derivatives for a Circular Plate

Axis position		Values of $-z_{\dot\theta}$			$-z_q$	Values of $-m_{\dot\theta}$			$-m_q$
	x_0/R	Multhopp $m = 5$	Multhopp $m = 7$	Ref. 5	Steady $m = 7$	Multhopp $m = 5$	Multhopp $m = 7$	Ref. 5	Steady $m = 7$
L.E.	0	2·136	2·113	2·087	1·364	1·900	1·888	1·904	1·112
	0·25	1·912	1·890	1·864	1·140	1·316	1·310	1·331	0·720
	0·50	1·688	1·666	1·642	0·917	0·844	0·843	0·869	0·441
	0·75	1·464	1·443	1·419	0·693	0·484	0·487	0·519	0·273
	1·00	1·240	1·219	1·196	0·470	0·236	0·244	0·279	0·217
	1·25	1·016	0·996	0·974	0·247	0·100	0·112	0·152	0·272
	1·50	0·782	0·772	0·751	0·023	0·077	0·092	0·135	0·440
	1·75	0·568	0·549	0·528	−0·200	0·165	0·184	0·230	0·719
T.E.	2·00	0·343	0·325	0·305	−0·424	0·366	0·387	0·436	1·109

Note: For a circular plate $C_L = L/\frac{1}{2}\rho U^2 S$, $C_m = \mathscr{M}/\frac{1}{2}\rho U^2 S\bar{c}$ where $S = \pi R^2$ and $\bar{c} = \frac{1}{2}\pi R$; and the derivatives are defined to be $z_{\dot\theta} = -\frac{1}{2}\partial C_L/\partial(\dot\theta R/U)$, $m_{\dot\theta} = (\bar{c}/2R)\,\partial C_m/\partial(\dot\theta R/U)$.

TABLE 3

Pitching Derivatives for an Arrowhead Wing ($A = 1\cdot32$)

Axis position		Values of $-z_\theta$			$-z_q$	Values of $-m_\theta$			$-m_q$
	$x_0/\bar{c}$	Multhopp		Ref. 5	Steady	Multhopp		Ref. 5	Steady
		$m = 5$	$m = 11$		$m = 11$	$m = 5$	$m = 11$		$m = 11$
Apex	0	1·644	1·546	1·528	1·241	1·802	1·727	1·708	1·379
	0·2	1·474	1·382	1·361	1·076	1·345	1·288	1·277	1·001
	0·4	1·303	1·217	1·194	0·912	0·957	0·916	0·912	0·689
	0·6	1·133	1·053	1·028	0·747	0·638	0·608	0·614	0·444
	0·8	0·962	0·888	0·861	0·583	0·386	0·367	0·383	0·263
	1·0	0·792	0·724	0·695	0·418	0·202	0·192	0·218	0·149
	1·2	0·621	0·559	0·528	0·254	0·087	0·082	0·120	0·100
	1·4	0·451	0·395	0·362	0·090	0·040	0·038	0·089	0·117
	1·6	0·280	0·230	0·195	−0·075	0·061	0·060	0·124	0·200
	1·8	0·110	0·066	0·029	−0·239	0·150	0·148	0·225	0·349
Kink at T.E.	2·1	−0·146	−0·181	−0·221	−0·486	0·412	0·403	0·503	0·696

TABLE 4

Pitching Derivatives for a Delta Wing ($A = 3$)

Axis position		Values of $-z_\theta$			$-z_q$	Values of $-m_\theta$			$-m_q$
	$x_0/\bar{c}$	Multhopp		Ref. 5	Steady	Multhopp		Ref. 5	Steady
		$m = 7$	$m = 15$		$m = 15$	$m = 7$	$m = 15$		$m = 15$
Apex	0	2·597	2·546	2·423	2·300	2·718	2·719	2·623	2·408
	0·25	2·213	2·165	2·038	1·919	1·812	1·822	1·760	1·573
	0·50	1·829	1·784	1·654	1·538	1·098	1·116	1·089	0·928
	0·75	1·445	1·402	1·269	1·157	0·576	0·600	0·610	0·474
	1·00	1·062	1·021	0·884	0·775	0·246	0·276	0·324	0·210
	1·25	0·678	0·640	0·500	0·394	0·109	0·141	0·231	0·138
	1·50	0·294	0·258	0·115	0·013	0·163	0·198	0·329	0·255
T.E.	1·75	−0·090	−0·123	−0·270	−0·369	0·409	0·445	0·621	0·564

TABLE 5

Pitching Derivatives for a Family of Delta Wings

Present Theory ($m = 7$)

Axis position		Values of $-z_{\dot\theta}$			Values of $-m_{\dot\theta}$		
	$x_0/\bar{c}$	$A = 3$	$A = 2$	$A = 1\cdot2$	$A = 3$	$A = 2$	$A = 1\cdot2$
Apex	0	2·597	2·241	1·662	2·718	2·422	1·870
	0·25	2·213	1·942	1·459	1·812	1·655	1·306
	0·50	1·829	1·644	1·256	1·098	1·038	0·843
	0·75	1·445	1·346	1·053	0·576	0·569	0·482
	1·00	1·062	1·047	0·850	0·246	0·250	0·222
	1·25	0·678	0·749	0·647	0·109	0·080	0·064
	1·50	0·294	0·450	0·445	0·163	0·059	0·008
T.E.	1·75	−0·090	0·152	0·242	0·409	0·187	0·052

TABLE 6

Pitching Derivatives for a Delta Wing ($A = 3$)
at $M = 0, 0\cdot745, 0\cdot917$

Present Theory ($m = 7$)

Axis position		Values of $-z_{\dot\theta}$			Values of $-m_{\dot\theta}$		
	$x_0/\bar{c}$	$M = 0$	$M = 0\cdot745$	$M = 0\cdot917$	$M = 0$	$M = 0\cdot745$	$M = 0\cdot917$
Apex	0	2·597	2·810	2·797	2·718	3·181	3·614
	0·25	2·213	2·362	2·289	1·812	2·169	2·543
	0·50	1·829	1·914	1·782	1·098	1·380	1·726
	0·75	1·445	1·467	1·274	0·576	0·815	1·163
	1·00	1·062	1·019	0·767	0·246	0·474	0·854
	1·25	0·678	0·572	0·260	0·109	0·357	0·799
	1·50	0·294	0·124	−0·248	0·163	0·463	0·997
T.E.	1·75	−0·090	−0·323	−0·755	0·409	0·793	1·448

TABLE 7

Out-of-phase Incidence Induced by In-phase Loading

Calculated values of α_3' (at $0 \cdot 9045c$)

Wing	Circle	Circle	Arrowhead	Arrowhead	Δ (A = 3)	Δ (A = 3)	Δ (A = 2)	Δ (A = 1·2)
η	m = 5	m = 7	m = 5	m = 11	m = 7	m = 15	m = 7	m = 7
0	0·849	0·850	1·021	1·112	1·040	1·184	1·172	1·247
0·1951						0·646		
0·2588				0·663				
0·3827		0·742			0·289	0·234	0·455	0·573
0·5000	0·663		0·370	0·267				
0·5556						−0·094		
0·7071		0·424		−0·031	−0·299	−0·326	−0·179	−0·067
0·8315						−0·496		
0·8660	0·121		−0·225	−0·201				
0·9239		−0·098			−0·592	−0·584	−0·549	−0·488
0·9659				−0·351				
0·9808						−0·621		

Calculated values of α_3'' (at $0 \cdot 3455c$)

Wing	Circle	Circle	Arrowhead	Arrowhead	Δ (A = 3)	Δ (A = 3)	Δ (A = 2)	Δ (A = 1·2)
η	m = 5	m = 7	m = 5	m = 11	m = 7	m = 15	m = 7	m = 7
0	0·191	0·178	0·278	0·369	0·247	0·327	0·349	0·415
0·1951						−0·093		
0·2588				0·037				
0·3827		0·122			−0·233	−0·346	−0·138	−0·046
0·5000	0·091		−0·167	−0·238				
0·5556						−0·528		
0·7071		−0·050		−0·441	−0·543	−0·640	−0·500	−0·430
0·8315						−0·716		
0·8660	−0·228		−0·603	−0·572				
0·9239		−0·377			−0·715	−0·750	−0·717	−0·691
0·9659				−0·717				
0·9808						−0·777		

Note: To the first order in frequency ω the in-phase loading corresponds to a uniform incidence Q. This induces an angle of upwash of amplitude $\omega \bar{c} Q \alpha_3 / U(1 - M^2)$ out of phase with the pitching motion.

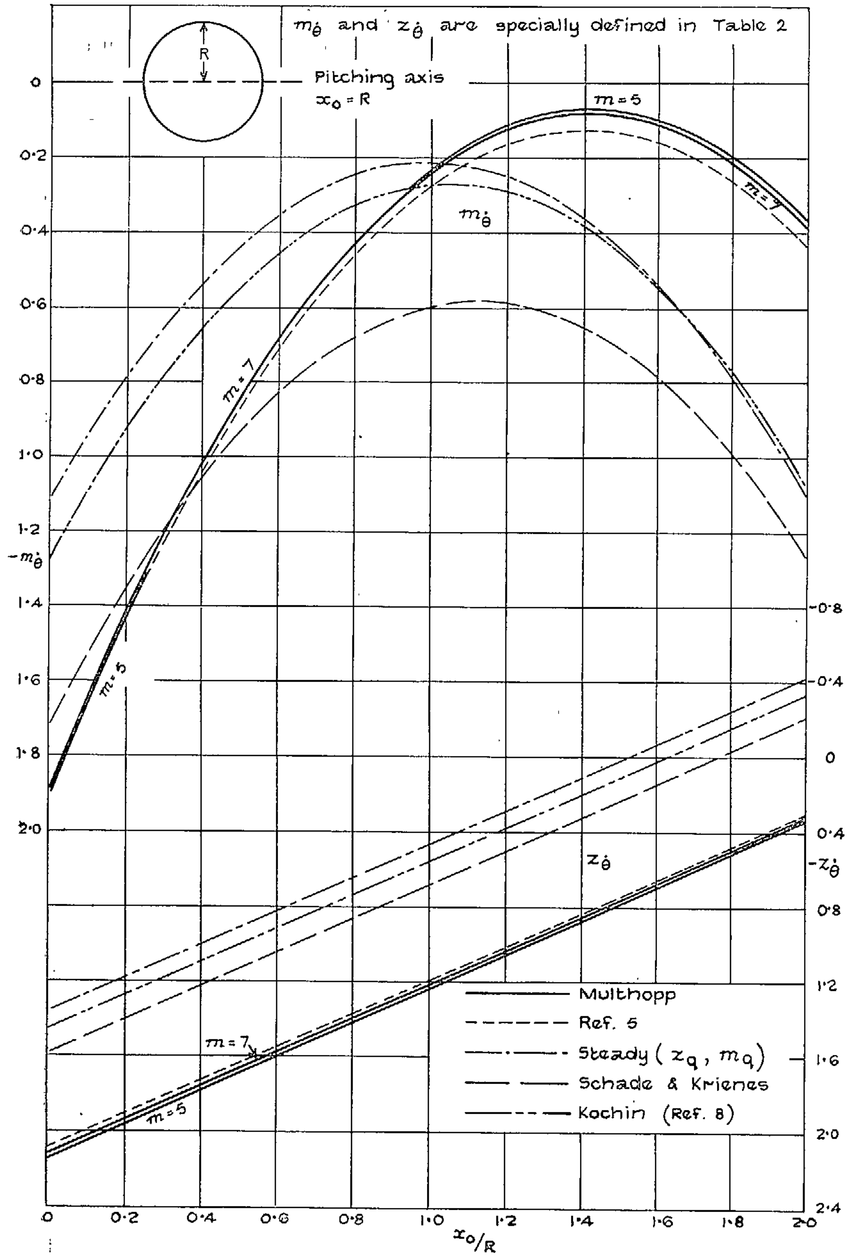

FIG. 1. Comparative theoretical values of m_{θ} and z_{θ} for a circular plate.

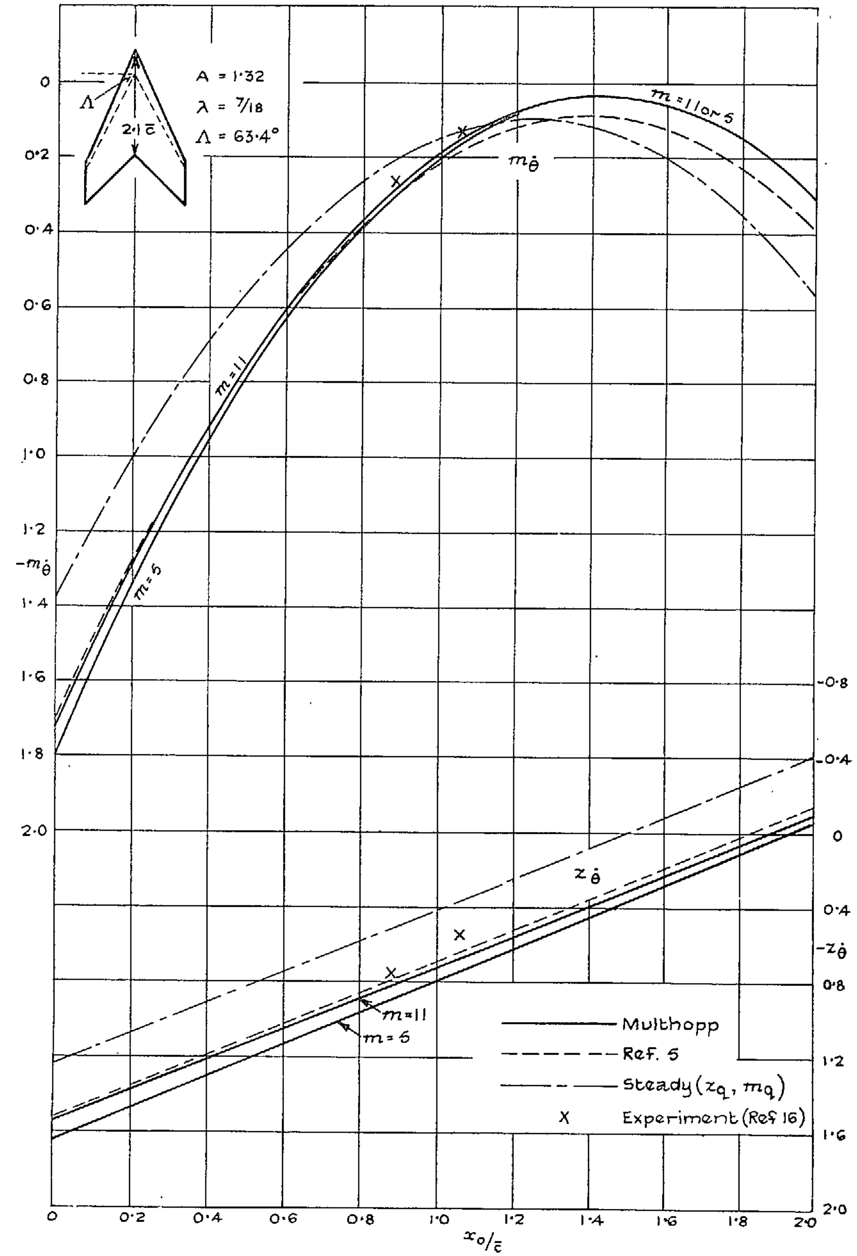

FIG. 2. Comparative theoretical and experimental values of m_{θ} and z_{θ} for an arrowhead wing.

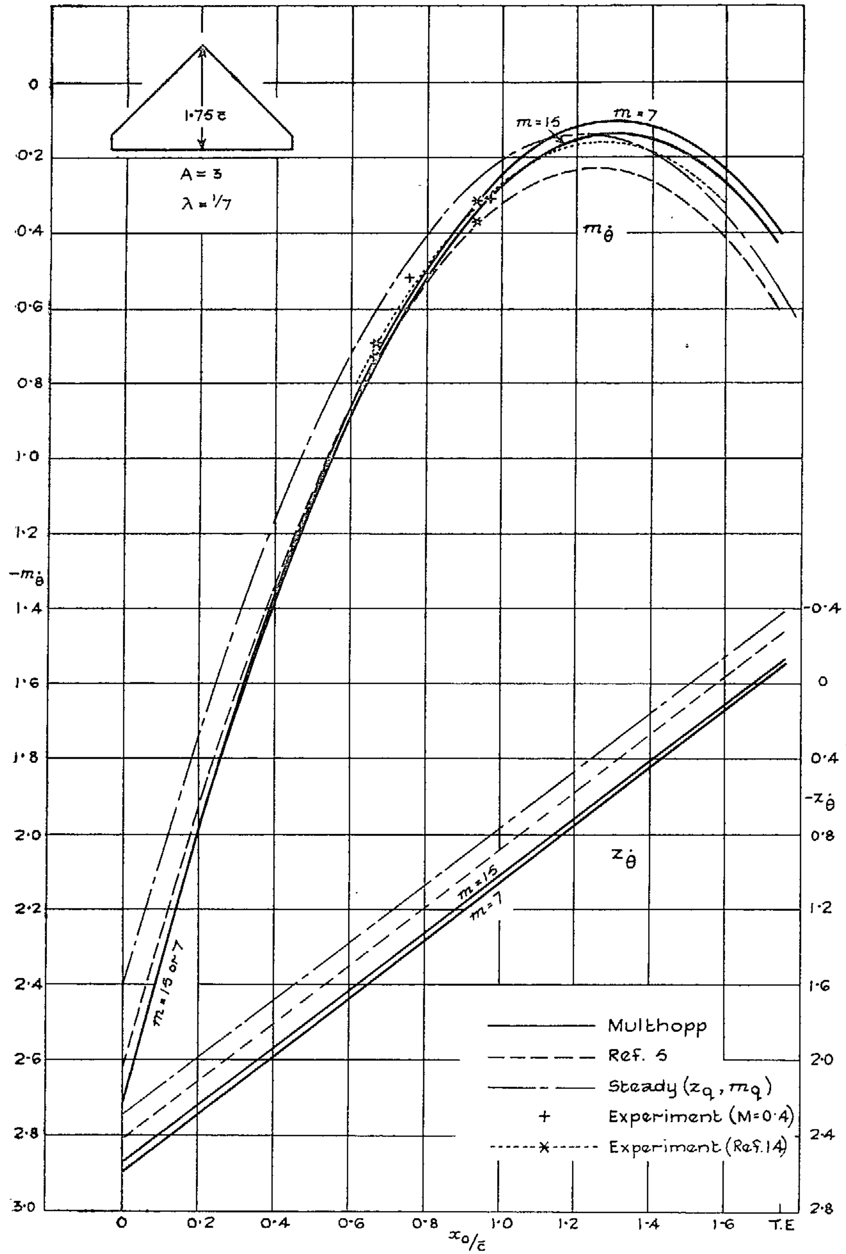

FIG. 3. Comparative theoretical and experimental values of $m_{\dot\theta}$ and $z_{\dot\theta}$ for a delta wing.

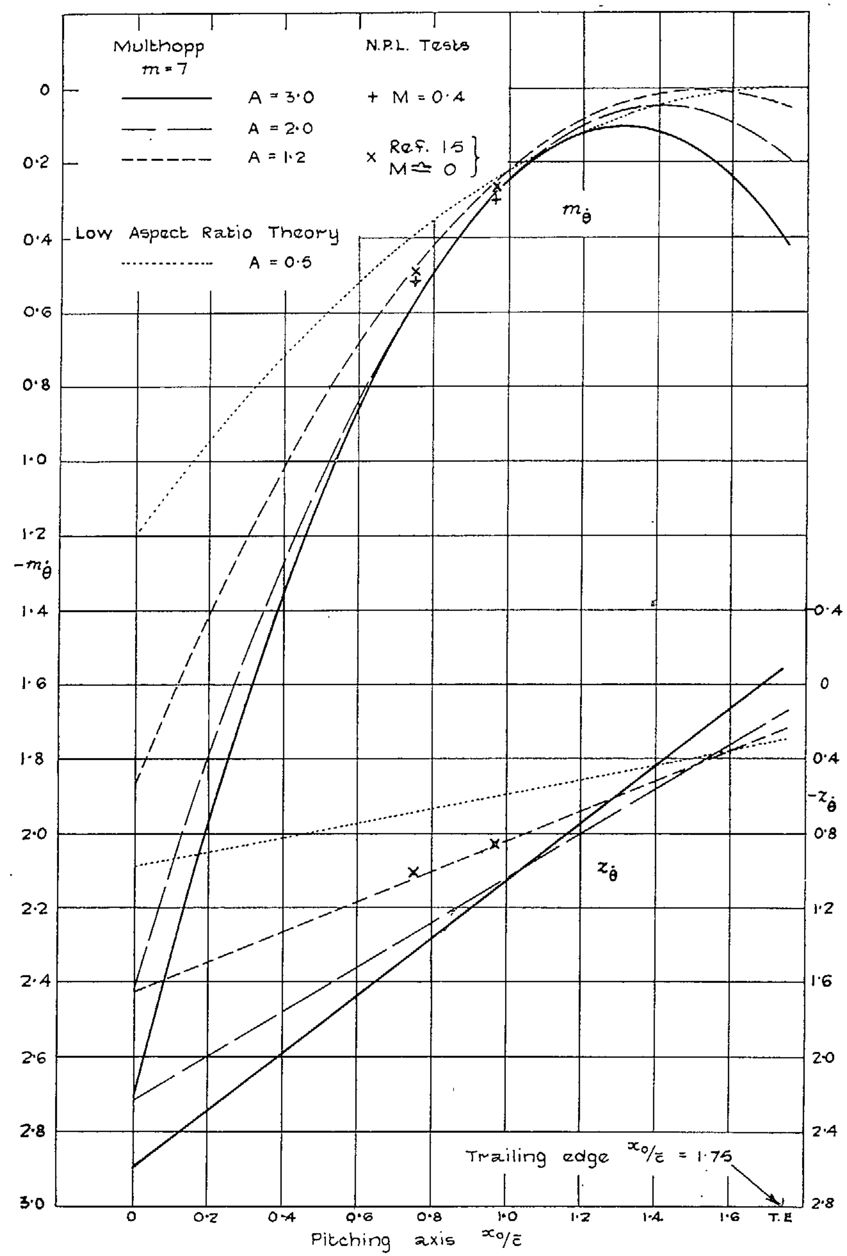

FIG. 4. Effect of aspect ratio on $m_{\dot\theta}$ and $z_{\dot\theta}$ for delta wings ($\lambda = 1/7$) in incompressible flow.

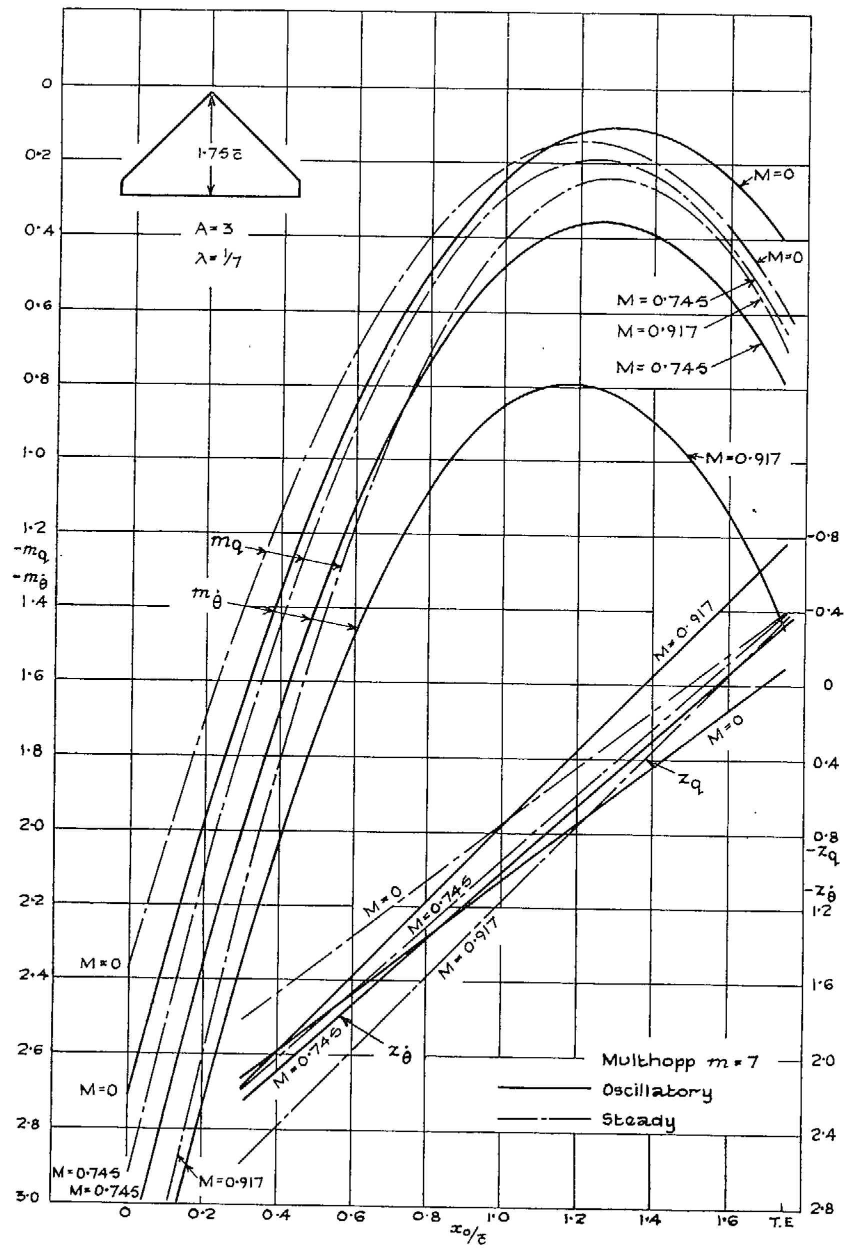

FIG. 5. Theoretical steady and oscillatory pitching derivatives for a delta wing at $M = 0, 0 \cdot 745, 0 \cdot 917$.

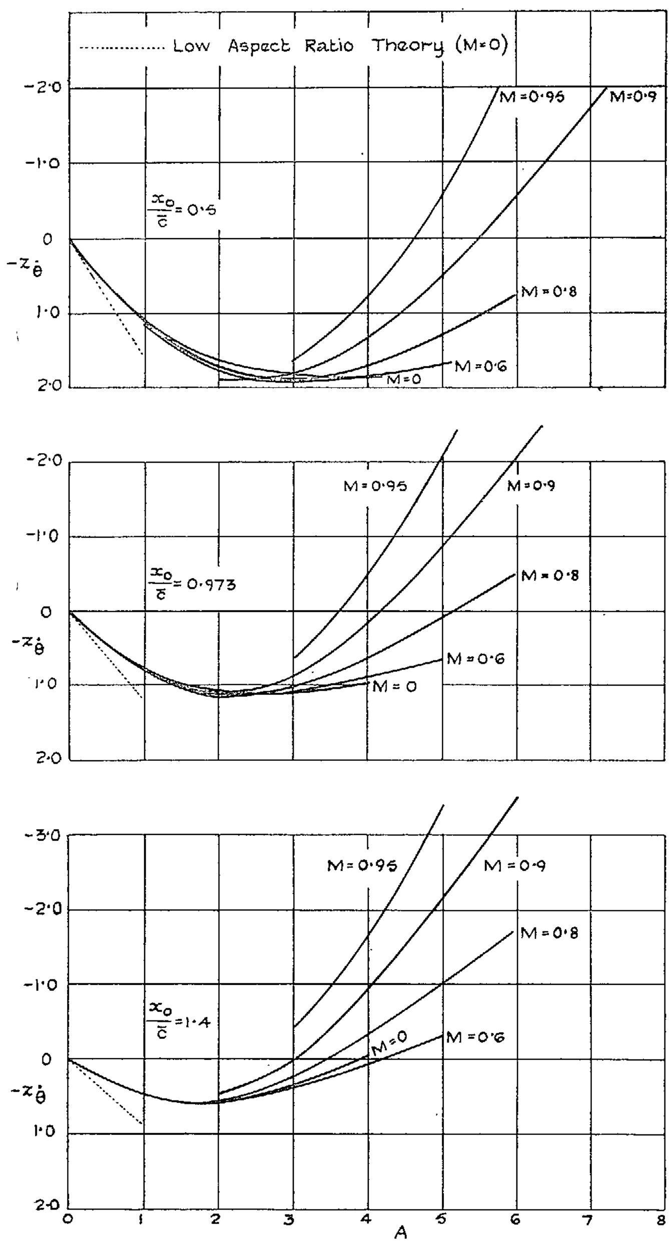

FIG. 6. Theoretical variation of $z_{\dot\theta}$ with aspect ratio for delta wings ($\lambda = 1/7$) with various pitching axes and Mach numbers.

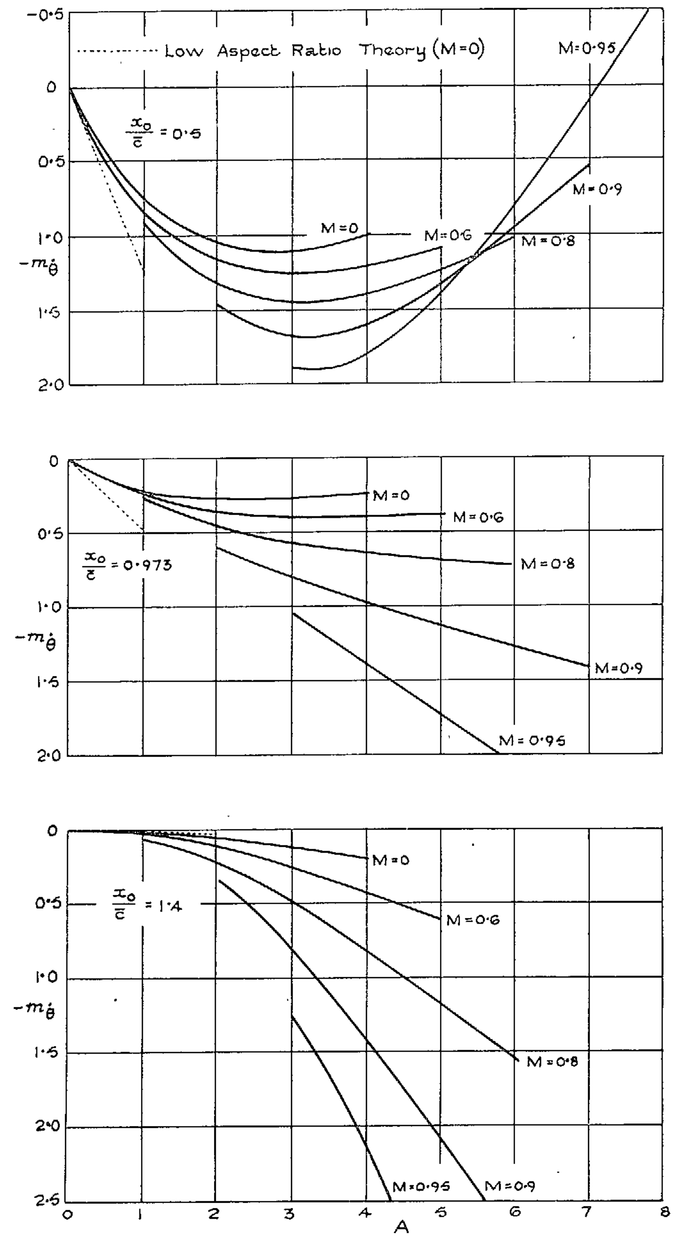

FIG. 7. Theoretical variation of $m_{\dot\theta}$ with aspect ratio for delta wings ($\lambda = 1/7$) with various pitching axes and Mach numbers.

D
J4335 18/9296 K7 2/56 D&Co. 34/263

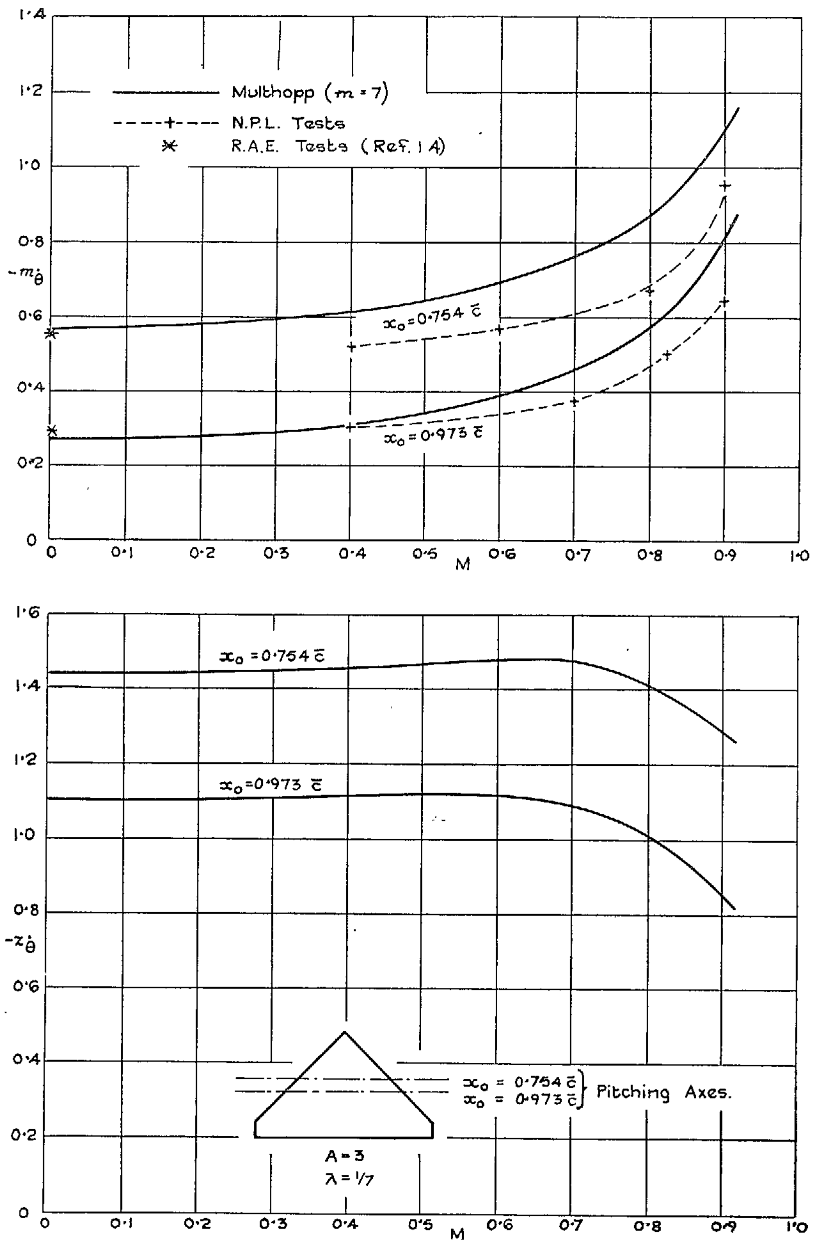

FIG. 8. Effect of compressibility on $m_{\dot{\theta}}$ and $z_{\dot{\theta}}$ for a delta wing with two pitching axes.

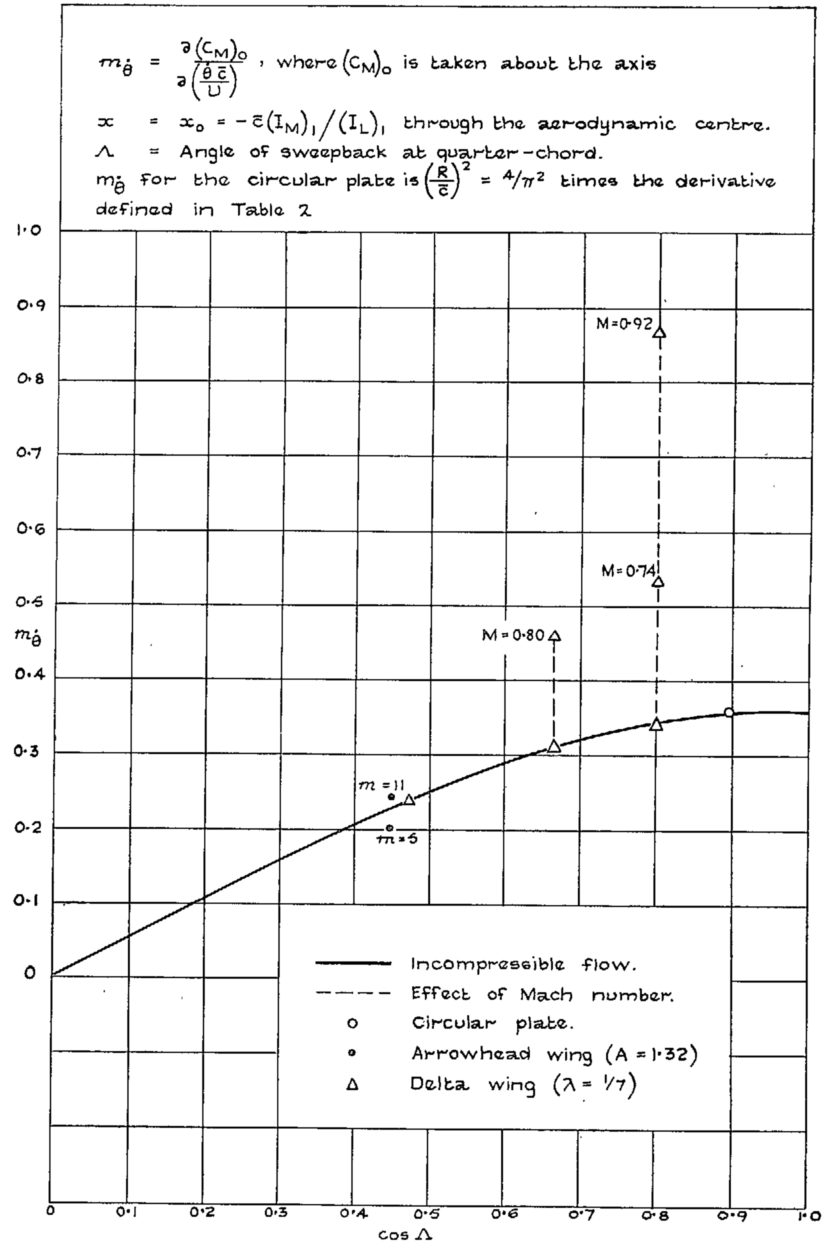

FIG. 9. Damping of pitching oscillations about the aerodynamic centre.

PRINTED IN GREAT BRITAIN

Publications of the Aeronautical Research Council

ANNUAL TECHNICAL REPORTS OF THE AERONAUTICAL RESEARCH COUNCIL (BOUND VOLUMES)

1938 Vol. I. Aerodynamics General, Performance, Airscrews. 50s. (51s. 8d.)
Vol. II. Stability and Control, Flutter, Structures, Seaplanes, Wind Tunnels, Materials. 30s. (31s. 8d.)

1939 Vol. I. Aerodynamics General, Performance, Airscrews, Engines. 50s. (51s. 8d.)
Vol. II. Stability and Control, Flutter and Vibration, Instruments, Structures, Seaplanes, etc. 63s. (64s. 8d.)

1940 Aero and Hydrodynamics, Aerofoils, Airscrews, Engines, Flutter, Icing, Stability and Control, Structures, and a miscellaneous section. 50s. (51s. 8d.)

1941 Aero and Hydrodynamics, Aerofoils, Airscrews, Engines, Flutter, Stability and Control, Structures. 63s. (64s. 8d.)

1942 Vol. I. Aero and Hydrodynamics, Aerofoils, Airscrews, Engines. 75s. (76s. 8d.)
Vol. II. Noise, Parachutes, Stability and Control, Structures, Vibration, Wind Tunnels. 47s. 6d. (49s. 2d.)

1943 Vol. I. Aerodynamics, Aerofoils, Airscrews. 80s. (81s. 8d.)
Vol. II. Engines, Flutter, Materials, Parachutes, Performance, Stability and Control, Structures. 90s. (91s. 11d.)

1944 Vol. I. Aero and Hydrodynamics, Aerofoils, Aircraft, Airscrews, Controls. 84s. (86s. 9d.)
Vol. II. Flutter and Vibration, Materials, Miscellaneous, Navigation, Parachutes, Performance, Plates and Panels, Stability, Structures, Test Equipment, Wind Tunnels. 84s. (86s. 9d.)

ANNUAL REPORTS OF THE AERONAUTICAL RESEARCH COUNCIL—

1933–34	1s. 6d. (1s. 8½d.)	1937	2s. (2s. 2½d.)
1934–35	1s. 6d. (1s. 8½d.)	1938	1s. 6d. (1s. 8½d.)
April 1, 1935 to Dec. 31, 1936	4s. (4s. 5½d.)	1939–48	3s. (3s. 3½d.)

INDEX TO ALL REPORTS AND MEMORANDA PUBLISHED IN THE ANNUAL TECHNICAL REPORTS, AND SEPARATELY—

April, 1950 – – – – – R. & M. No. 2600. 2s. 6d. (2s. 7½d.)

AUTHOR INDEX TO ALL REPORTS AND MEMORANDA OF THE AERONAUTICAL RESEARCH COUNCIL—

1909–January, 1954 – – – R. & M. No. 2570. 15s. (15s. 5½d.)

INDEXES TO THE TECHNICAL REPORTS OF THE AERONAUTICAL RESEARCH COUNCIL—

December 1, 1936 — June 30, 1939.	R. & M. No. 1850.	1s. 3d. (1s. 4½d.)
July 1, 1939 — June 30, 1945. –	R. & M. No. 1950.	1s. (1s. 1½d.)
July 1, 1945 — June 30, 1946. –	R. & M. No. 2050.	1s. (1s. 1½d.)
July 1, 1946 — December 31, 1946.	R. & M. No. 2150.	1s. 3d. (1s. 4½d.)
January 1, 1947 — June 30, 1947. –	R. & M. No. 2250.	1s. 3d. (1s. 4½d.)

PUBLISHED REPORTS AND MEMORANDA OF THE AERONAUTICAL RESEARCH COUNCIL—

Between Nos. 2251–2349. – –	R. & M. No. 2350.	1s. 9d. (1s. 10½d.)
Between Nos. 2351–2449. – –	R. & M. No. 2450.	2s. (2s. 1½d.)
Between Nos. 2451–2549. – –	R. & M. No. 2550.	2s. 6d. (2s. 7½d.)
Between Nos. 2551–2649. – –	R. & M. No. 2650.	2s. 6d. (2s. 7½d.)

Prices in brackets include postage

HER MAJESTY'S STATIONERY OFFICE

York House, Kingsway, London W.C.2; 423 Oxford Street, London W.1 (Post Orders: P.O. Box 569, London S.E.1); 13a Castle Street, Edinburgh 2; 39 King Street, Manchester 2; 2 Edmund Street, Birmingham 3; 109 St. Mary Street, Cardiff; Tower Lane, Bristol 1; 80 Chichester Street, Belfast, *or through any bookseller*

S.O. Code No. 23-2885

R. & M. No. 2885